Chapter 1. Introduction

1.1 History and background of magnetism

The history of science begins with the history of magnetism. Magnetic materials has attracted people since Thales of Miletus in 634-546 BC first demonstrated the phenomena as the lodestone, which is a natural mineral magnetite (Fe_3O_4) attract iron. Over the last 2,500 years mankind has extensively used magnetic materials for navigation, high tech applications and power production. It has procured so much well-known implying that, following Thales of Miletus, attraction and magnetism are utilized synonymously. Any point by point scientific clarification often enters mystical domain exemplified by the idea of spin that emerged from Dirac's relativistic treatment of an electron in an outer electromagnetic field. It has turned into the set up scientific idea and we construct our comprehension of magnetism on the electronic spin, which offers ascend to the spin magnetic moment, and the movement of electric charges and the related orbital magnetic moment [1].

The most primitive magnetic phenomena were experienced before the beginning of recorded history, and magnetism is one of the earliest field in physics. Pliny the Elder (23-79 AD) described, the origin of the name 'Magnet' in their "Historia Naturalis". The name magnet emerged from Magnes named shepherd, who found that his iron-nailed shoes stuck

to the ground when he was going around the grass field. It is also likely that the name emerged from Magnetes, the colonists of Magnesia in Asia Minor, who knew about the ore in the nearby area which attract Iron objects. Since about 1500 AD, the name lodestone has been utilized to depict such magnetic ore because of its application in navigation. In the modern world we connect lodestone with the spinel magnetite which is magnetically adjusted along Earth's magnetic field; this alignment is due to the impact of the earth's magnetic field during the cooling procedure of hot lava [1].

The first Chinese reference to magnetism is attributed to Guanzhong (645 BC) and later many more statements citing lodestone were mentioned in the Chinese literature. In China lodestone was called as "Cishi", the loving stone, because of its capability to attract iron [2]. The direction pointers, i.e., compasses were designed in the Qin dynasty (221-206 BC) by balancing a piece of lodestone on a bronze plate. A serving spoon made of lodestone was placed on a bronze plate in such a way that its handle pointed to the south. Rather than navigation, these compasses were also used for "feng-shui" or geomancy, the Chinese technique of acquiring harmony with the forces of nature [2]. Another interesting reference of a compass is found in the book "Meng Chhi Pi Than" (1086 AD) authored by Shen Kua, which not only shows the compass needle to point towards the south but also refers to a slight easterly deviation showing the declination of the compass [2]. Initially the Chinese have used the compass primarily for overland navigation; later about the end of the 12th century it appeared on their ships [2]. In Europe, first record of compass came in 1187 by the Englishman A. Neckam in his works "De utensilibus" and "De naturis rerum". The medieval European literature also reported about magnetic mountains or islands whose

magnetism was said to have the capacity to evacuate the copper or bronze nails out of boats. Around 1780, F. A. Mesmer found a mending strategy on the conviction that living bodies are magnetized and healed mesmerized by magnetic fields [1].

The compass was first used for mapping the magnetic force of a load stone by the French soldier Pierre de Maricourt in 1263. He found that a magnet had two poles, North Pole and South Pole. The compass was first utilized for directional navigation in western countries after AD 1200. The first attempt was made by the French scholar Petrus Peregrinus to explore the aspects of magnet in the 13^{th} century and his finding hold for approximately 300 years. In 1600, William Gilbert, an English physicist published his book on Magnet, "Magnetic bodies and the Great Magnet of the Earth". He was the first who applied different scientific methods to systematically explore different magnetic phenomena. The greatest contribution on the history of magnetism was made by Gilbert, who found that the earth itself carries on like a monster magnet [3-5]. He clearly differentiate the electricity and the magnetism. Quantitative investigations of magnetism has begun in the early of eighteenth century. A famous geologist John Michel (1724 - 1793) used to think about the magnetic forces by developing a balance in 1750. He demonstrated that the magnetic attraction and repulsion decreases as the increase in square of the distance from the poles. Charles Augustine de Coulomb (1736 - 1806), the French physicists had estimated the forces acting between electric charges. He also invented 'the inverse square law of force' between the electric charges and also between the magnetic poles. In this way, he checked John Michel's perception with high exactness [6].

In the beginning of the modern world, the impact of electric currents on magnetic compass was found by Oersted in 1820. From that point, in 1831 Faraday suggested the induction principle which offered ascend to another scientific discipline: electromagnetism [2]. In late 19^{th} and early 20^{th} century quantum mechanics and the special theory of relativity under veil of the Bohr's theory of the atom and the Dirac theory of the electronic spin explained atomic and electronic nature of perpetually circulating currents. The molecular field theory proposed by Weiss to explain the ferromagnetic order employed the quantum mechanics of Pauli and Heisenberg for a logical explanation [7].

The period 1905 - 1930 was the Age of digging deep. A radical approach proposed by Neel for magnetic phenomena, could successfully explained the hysteresis and the magnetism of magnetite and other oxides based on their crystal structure. Magnetism in the 1940s and 1950s focused on microwave and radio-frequency applications. As a consequence of this, nuclear and electronic magnetic resonance emerged as powerful methods of investigating solids and liquids. From 1960 onwards came an Age of Applications, when soft magnetic materials, proliferated in components for consumer goods, significantly enhancing their role in electronics and technology. However, magnetism particularly at nano-scale, continue to emerge, the great path-breaking technology of the age [7].

1.2 Magnetic moment due electronic spin

There are two types of electronic movement namely orbital and spin motion and there is a magnetic moment associated with both the motion of electron. The orbital motion of

an electron is similar to a current loop of wire without resistance, and both are circulating the charge.

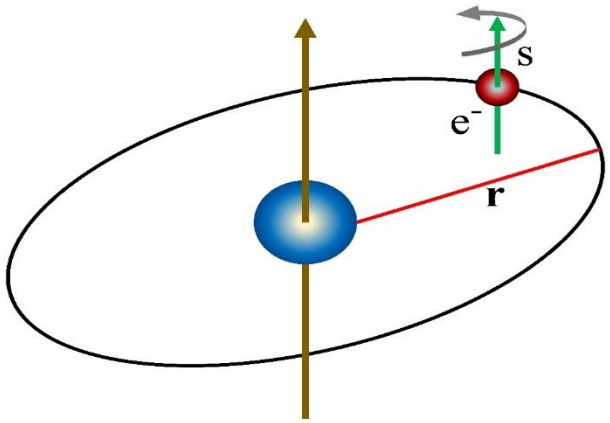

Fig. 1.1. Magnetic moment due electrons in atomic orbital.

Therefore, the magnetic moment associated with the orbital motion of an electron can be written as,

$$\mu = (\text{area of loop}) \times (\text{current}) \qquad (1.1)$$

If *e* is the electronic in *esu* and *c* is velocity of light, then *e/c* is the electronic charge in *emu*. The current or charge crossing through a particular point per unit time is thus

$$(e/c)(\frac{v}{2\pi r})$$

Therefore, the orbital magnetic moment is given by

$$\mu_{orbit} = \pi r^2 \left(\frac{ev}{2\pi rc}\right) = \frac{evr}{2c} \qquad (1.2)$$

The angular momentum of the electron can be written as

$$mvr = nh/2\pi \qquad (1.3)$$

Combining the last two equations, we get the orbital magnetic moment of an electron in the 1st Bohr orbit is

$$\mu_{orbit} = \frac{eh}{4\pi mc} \qquad (1.4)$$

Spinning is an exclusive property of electrons at any temperature in all conditions of matter. The electrons behave as if they were spinning about its own axis, as well as moving in an orbit around the nucleus. There is some definite amounts of magnetic moments and angular momentum associated to this spinning of electron. The magnetic moment due to that spinning of electron can be represent as,

$$\mu_{spin} = \frac{eh}{4\pi mc} \qquad (1.5)$$

where *e* is the charge on the electron, *h* is Planck's constant, *m* is the mass of electron and *c* is the velocity of light. Substituting all the values in above equation, the magnetic moment due to the spin and orbital motion of electrons are found to be equal to $0.927 \times 10^{-20}\ erg/Oe$. It is such a fundamental quantity that it was taken as a unit to measure magnetic moment. This is called Bohr-Magneton and specially symbolized as μ_B.

There are some fundamental concepts associated with the field of magnetism. Magnetic moment is one such term. The magnetic moment is defined as the couple act on a magnet, having pole strength *p* and length *l*, placed in a uniform magnetic field H at an angle θ. Hence, the moment *m* and is given by,

$$m = pHsin\theta\left(\frac{l}{2}\right) + pHsin\theta\left(\frac{l}{2}\right) = (pHsin\theta)l \quad (1.6)$$

If H = 1 Oe and θ = 90°,

$$m = pl \quad (1.7)$$

The magnetic moment per unit volume is called intensity of magnetization or simply magnetization and is given by,

$$M = \frac{m}{V} \quad (1.8)$$

;where V is the volume of the material. The specific magnetization is defined as,

$$\sigma = \frac{m}{W} = \frac{m}{v\rho} = \frac{M}{\rho}\ emu/g \quad (1.9)$$

;where W is the mass and ρ is the density of the material. The magnetic properties of a magnetic material are characterized by both the sign and magnitude of M and by the nature of variation of M with H [8].

The magnetization per unit magnetic field is called the magnetic susceptibility (χ), which can be expressed as

$$\chi = \frac{M}{H}\ emu/cm^3.Oe \quad (1.10)$$

The magnetization M of a material is described by the equation

$$B = \mu_0(H + M) = \mu_0\mu_r H = \mu H \quad (1.11)$$

;where $\mu_0 = 4\pi \times 10^{-7} H/m$ is the permeability of free space, *B* and *H* are recorded in Tesla (T) and Am^{-1} respectively and μ_r is called as the relative permeability of the material.

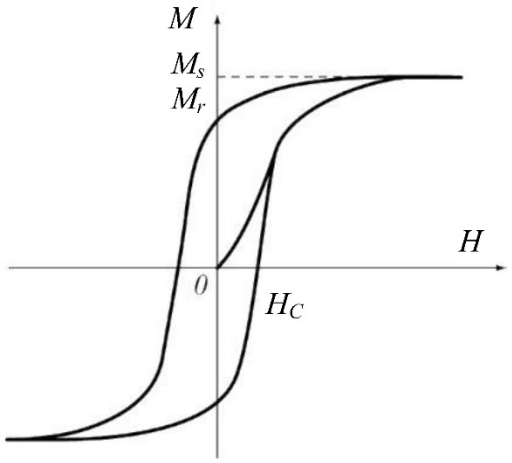

Fig. 1.2. Typical hysteresis loop of a magnetic material.

Hence, from the above equations, it can be shown that

$$\mu_r = (1 + \chi) \qquad (1.12)$$

The value of χ *and* μ_r characterizes the magnetic properties of a material.

Typical curves of *M* vs. *H* called magnetization curves are described by phenomena called saturation magnetization and hysteresis. At certain values of *H,* the magnetization M becomes saturate and have a value M_s. after saturation, as *H* decreases to zero, *M* does not decreases to zero which is called as hysteresis. M_r is the remanant magnetization and H_c is the coercivity or coercive field of the material, i.e., the negative field is to apply to decrease the magnetization to zero.

1.3 Magnetic Domain

The primary characteristic of ferromagnetic materials is the ordering of electronic spin, which gives rise to create a region of magnetic alignment, called domain. A Domain is described by a group of unidirectional electron spins acting collectively. The domain walls separate the domain walls. There is some energy related with the formation and presence of domain walls. For hard magnetic materials the typical value of domain-wall width is 5 *nm* and for soft magnetic materials the value is 100 *nm*. The domain-wall energy extend from 0.1 mJ/m^2 for soft magnetic materials to about 50 mJ/m^2 for hard magnetic materials [9].

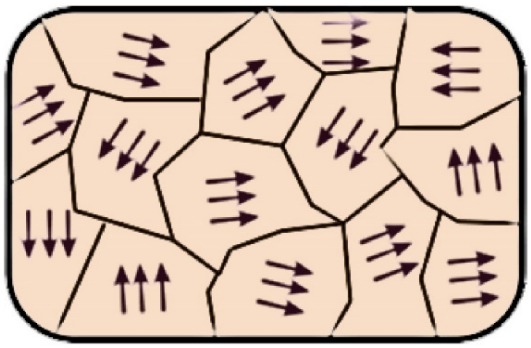

Fig. 1.3. Magnetic domains and domain wall.

There is a high degree of magnetization within individual domains. The domains are randomly oriented at zero external magnetic field. A small external magnetic field is enough for significant orientation of the magnetic domains. When there is a non-zero external magnetic field, there is growth of domains parallel to the applied field without reorienting the domain itself. Also there is shifting of the domain boundaries in favor of those domains which are parallel to the applied field. The internal magnetic fields arises as

a result of the long range ordering of the electronic spins. The internal magnetic fields are much stronger than the external magnetic fields, needed to perform the changes in domain alignment. The alignment of domains result in the amplification of the external magnetic which is expressed in terms of the relative permeability (μ_r) [10].

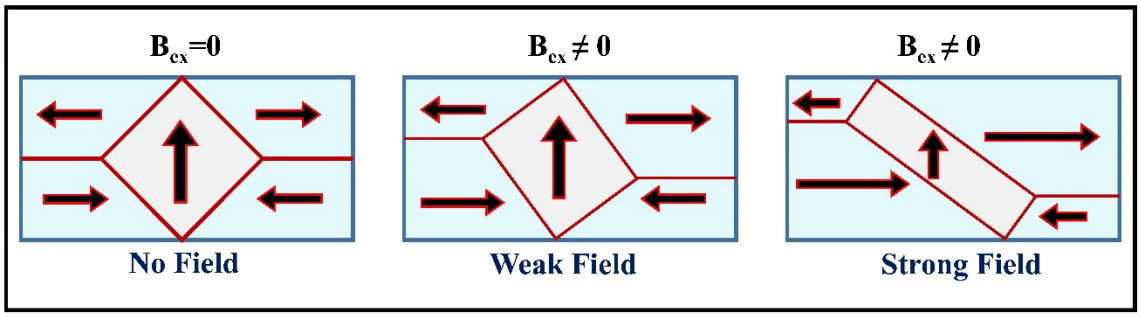

Fig. 1.4. Shifting of domain wall in favor of applied magnetic field.

1.4 Classification of magnetism

Different magnetic materials corresponds to different magnetic interactions and spin alignment, belongs to different kinds of magnetism which are depicted in figure 1.5.

Depending upon the magnetic behavior, magnetism can be classified into following classes

1.4.1 Diamagnetism

Diamagnetism is naturally present in all the materials, though it is very weak in nature. It arises by the virtue of non-cooperative behavior of electrons when the atom is kept in an external magnetic field. The net magnetic moment of the atoms in diamagnetic material is always zero, i.e., there is no unpaired electrons and all the orbitals are fully

filled. However, a negative magnetization is formed when an external magnetic field is applied, which results in a negative susceptibility. The negative susceptibility of the diamagnetic substances is of the order of 10^{-6}, which is temperature independent.

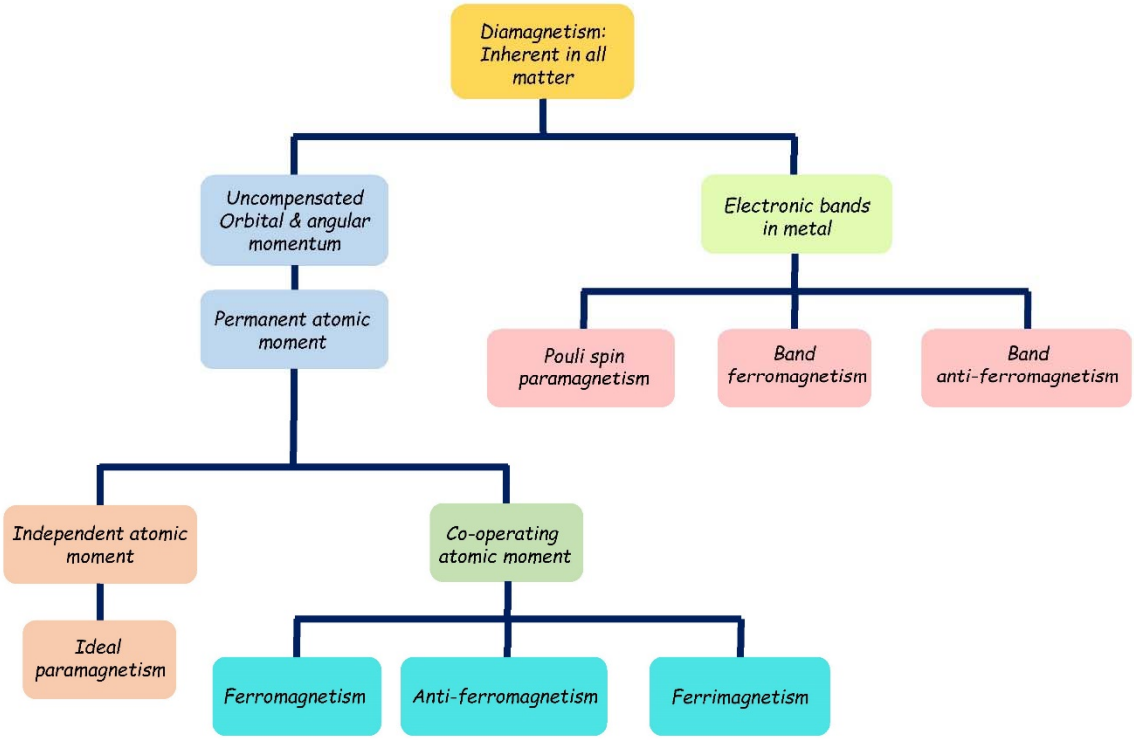

Fig. 1.5. Classification of magnetic materials.

The orbits of the electrons in the diamagnetic substances can be consider as a current loops. The magnetic moment induced in such atoms, ions and molecules is directly proportional to the electric current multiplied by the area of the current loop. Current will rely on the number of electrons times the electronic charge and on the frequency of the orbital movement, which additionally relies upon the charge *e*. Consequently, the

susceptibility is proportional to $Ze^2 <r^2>$;where r is the radius of orbit and Z is the atomic number of the element.

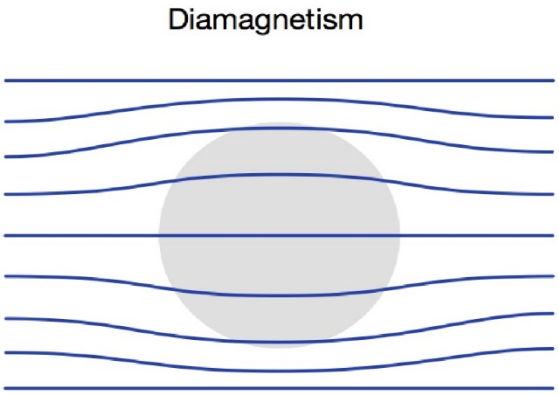

Fig. 1.6. Magnetic lines of force are excluded by diamagnetic material.

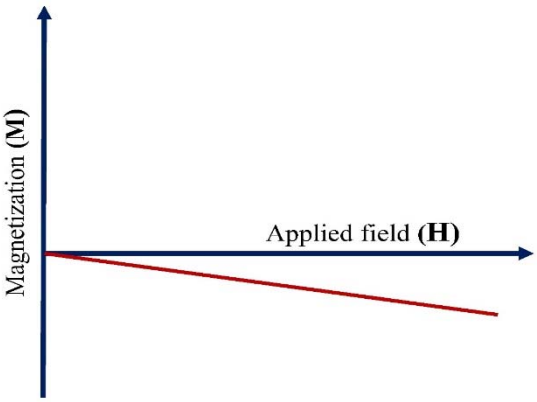

Fig. 1.7. M vs. H curve of diamagnetic material.

Langevin's theory suggested that the susceptibility of the diamagnetic material can be expressed as

$$\chi = -\frac{NZe^2}{mc^2} < r^2 > \qquad (1.13)$$

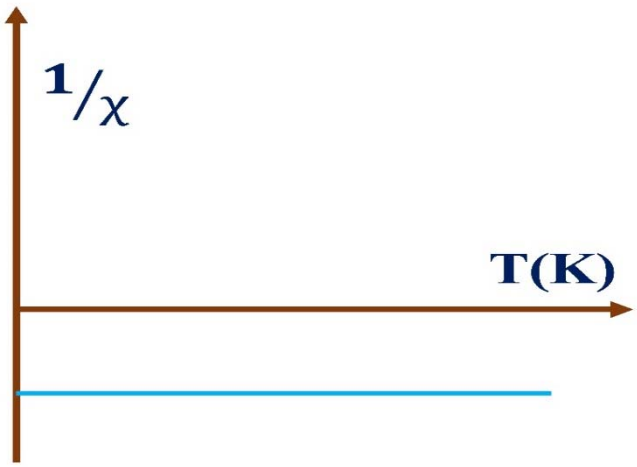

Fig. 1.8. Temperature variation of inverse susceptibility

;where, N is the atomic density, m is the electronic mass, and c is the speed of light. The other trademark conduct of diamagnetic material is that the susceptibility is temperature independent [8].

1.4.2 Paramagnetism

The materials undergo paramagnetism when there is a net magnetic moment associated with some or all of the atoms of the substance. The moments can align themselves in any direction if the interaction between them is negligible enough (Figure 1.9). This is called paramagnetism of free atoms. The presence of unpaired electrons in partly filled orbitals, net atomic magnetic moment is induced in paramagnetic. As an external magnetic field is applied, the moments can orient themselves to induce a non-zero magnetization along the direction of applied field.

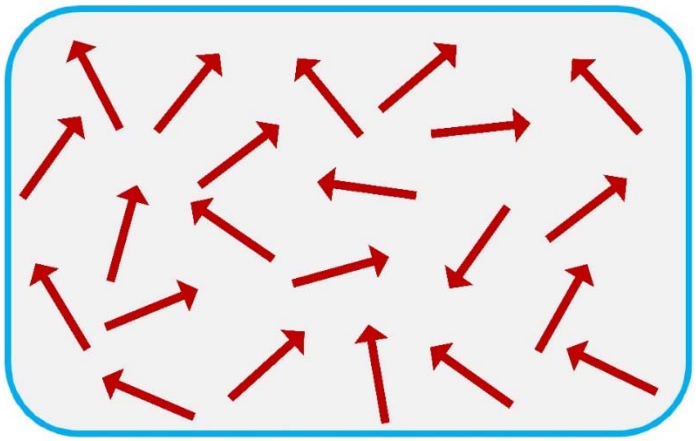

Fig. 1.9. Arrangement of individual magnetic moments in paramagnetic materials.

However, when there is no external magnetic field, the seperate magnetic moments are randomly oriented, hence, the net magnetization become zero as like as in the case of diamagnetism. But when the field is applied, there is a partial orientation of atomic

magnetic moments along the direction of field. Hence there induced a net positive magnetization and therefore the positive susceptibility.

In limited fields and at room temperature, the susceptibility of the paramagnetic materials are low, but higher than the diamagnetic commitment. The theory of paramagnetism given by Langevin successfully explains, how the magnetic properties of a paramagnetic substance depends on temperature.

The Langevin theory interpreted that the total magnetic moment of paramagnetic material is

$$M = NmL(x) \tag{1.14}$$

$$L(x) = \{\coth(x) - \frac{1}{x}\} \tag{1.15}$$

Where $x = \frac{mH}{k_B T}$ (1.16)

;where, *N* is the number of atoms, *m* is the magnetic moment of each atom, *L(x)* is called the Langevin function, *H* is the magnetic field applied, k_B is the Boltzmann's constant and *T* is the absolute temperature.

When *x* is very small, i.e. when $k_B T \gg mH$

$$L(x) \cong \frac{x}{3} \tag{1.17}$$

Hence the magnetization can be expressed as

$$M \cong \frac{Nm^2 H}{3k_B T} \tag{1.18}$$

The result shows that the susceptibility varies with inverse temperature which is known as the Curies law (figure 1.11) expressed as

$$\chi = \frac{M}{H} = \frac{C}{T} \qquad (1.19)$$

;where C is the Curie constant can be written as

$$C = \frac{Nm^2}{3k_B} \qquad (1.20)$$

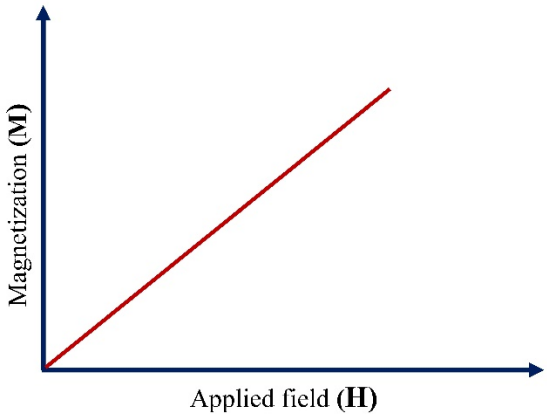

Fig. 1.10. M vs. H curve of paramagnetic material.

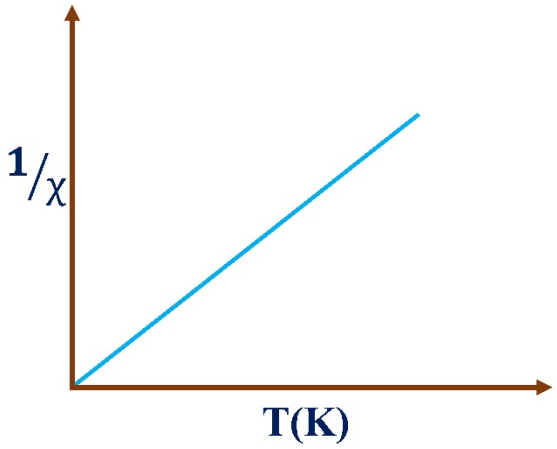

Fig. 1.11. Temperature variation of inverse susceptibility of paramagnetic substance.

At large *x,* $L(x) \rightarrow 1$, and all moments are aligned along the direction of applied magnetic field. This is known as saturation magnetization,

$$M_S = Nm \qquad (1.21)$$

If we consider the quantum mechanical effects in magnetism, then the resultant magnetic moment is given by

$$M = NgJ\mu_B B_J(x) \tag{1.22}$$

Where $$B_J(x) = \frac{2J+1}{2J}\coth\left\{\frac{(2J+1)x}{2J}\right\} - \frac{1}{2J}\coth(\frac{x}{2J}) \tag{1.23}$$

And $$x = \frac{gJ\mu_B H}{k_B T} \tag{1.24}$$

The function B_J (x) is referred as the Brillouin function .And the function have two limits with *J*.

When $J = \frac{1}{2}$, $$M = Nm\{tanh(x)\} \tag{1.25}$$

And when $J \to \propto$, the Brillouin function will be the Langevin function.

The paramagnetic theory reveals that the magnetization data for a paramagnet fall on an all-inclusive curve if plotted as a component of H/T. The variation of (1/χ) with temperature for paramagnetic material gives a straight line. But the experimental data of paramagnetic materials shows that there is a deviation from Curie's law particularly at low temperature. This deviation is mainly due to the contribution of Van Vleck's paramagnetisam. In metals, due to the conduction of electrons, there induced a paramagnetic behavior, which is known as Pauli paramagnetism. The susceptibility associated with Pauli paramagnetism, is independent of temperature [8].

1.4.3 Ferromagnetism

One of the unique property of some magnetic materials is Ferromagnetism. Some materials like iron, cobalt, nickel etc. exhibit spontaneous magnetization even if without any applied magnetic field. This spontaneous magnetization is due to very strong

interactions between the atomic magnetic moments in the materials. Such magnetic is mainly directed by the magnetic exchange interactions [8, 11-13]. The electronic exchange forces produces the interactions for the parallel or antiparallel orientation of atomic moments. The positive exchange interactions is responsible for parallel ordering, whereas the negative exchange interaction is responsible for antiparallel ordering of magnetic moments in neighboring atoms. For ferromagnetic materials, the susceptibility becomes infinite at a certain temperature, known as the Curie temperature T_C, instead of become infinite at 0K as in the case of paramagnet. Below the Curie temperature the interactions overwhelm the thermal disturbance and a spontaneous magnetization induced when there is an external magnetic field. At 0K the spontaneous magnetization turns into its estreme value M_0 due to alignment of all the individual moments.

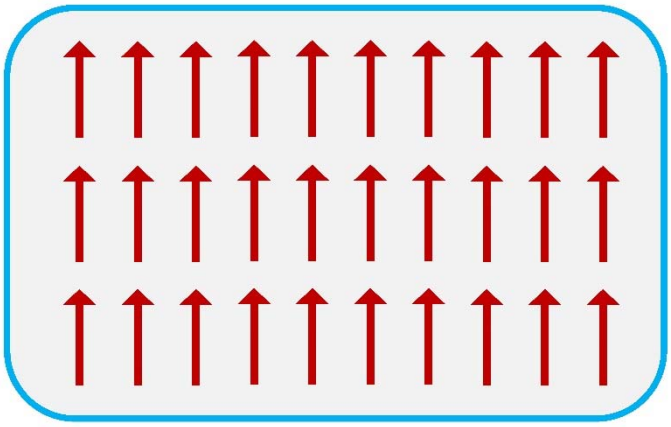

Fig. 1.12. Arrangement of individual magnetic moments in ferromagnetic materials.

Therefore the ferromagnetic materials are found to show an altered temperature reliance of χ which is depicted by the condition

$$\chi = \frac{C}{T-\theta} \qquad (1.26)$$

;where θ is a critical temperature which may have both positive or negative values. This is regarded as Curie Weiss Law. On account of ferromagnet this temperature is known as the ferromagnetic Curie temperature. In light of the magnetic interactions among the atomic moments the law was created by considering the Weiss molecular field theory.

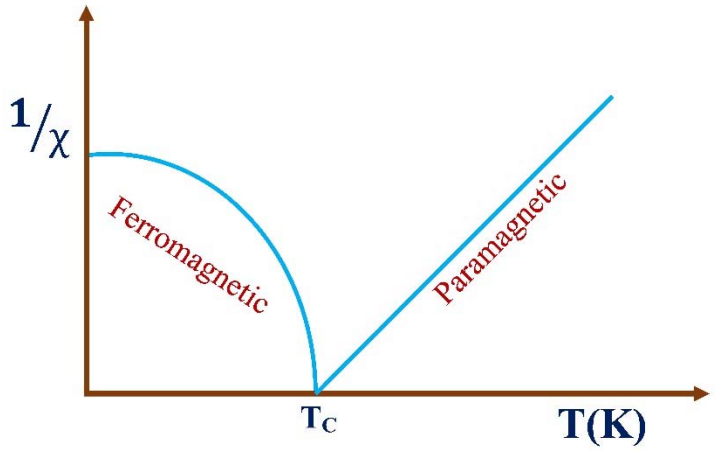

Fig. 1.13. Temperature variation of inverse susceptibility of ferromagnetic substance.

Considering the Weiss molecular field theory, a molecular field acted upon on a ferromagnetic material below the Curie temperature and also in the paramagnetic region above T_C and this molecular field is sufficient enough to magnetize the material even if there is no external field. To show this association he accepted that the net interaction on a given magnetic moment is a viable magnetic field, a mean field because of every other moments. Anyway the temperature reliance of χ produce a very large values for the molecular field and consequently the theory was found to have some difficult issues. Therefore more precise speculations consider the only nearest neighbor interactions to find

the atomic magnetic moments. This interactions are due to exchange interaction, rather than magnetic, which is based on quantum mechanical origin.

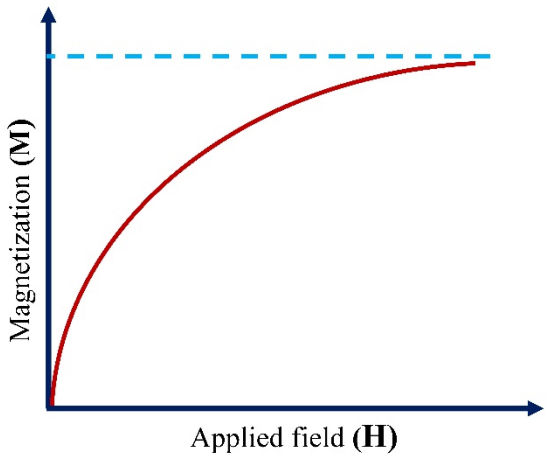

Fig. 1.14. The variation of magnetization with applied field of ferromagnetic material.

The genuine physical source of the exchange interaction was evaluated by Heisenberg. Quantum mechanics accommodates for an exchange interaction between two atoms in light of symmetry, the Pauli's exclusion principle and the Coulombic interaction. Heisenberg demonstrated that the exchange interaction between two electrons produced an exchange energy between neighboring spins can be written as

$$E_{ex} = -2J_{ex}S_i.S_j \qquad (1.27)$$

;where, S_i and S_j spin of neighboring electrons and J_{ex} is known as the exchange integral. If J_{ex} have the positive value, this describes the configuration with lower energy leads to parallel magnetic moments as in the case of ferromagnetism. If *Jex* have the negative value, leads to antiparallel allignment.

There are two theories which are utilized to explain the origin of ferromagnetism in metals: (i) theory of localized moment (ii) band theory associated with the confined moment theory. The valence electrons can't move about the crystal as they are appended to the atoms. A magnetic moment is contributed by these valence electrons which are confined in an atom. Therefore the dependence of spontaneous magnetization with temperature in ferromagnetic region can be interpreted based on the localized moment theory. This theory also illustrate the Curie Weiss law above T_C. Now in the case of band theory, the electrons are not attached to atoms rather than it can move freely thoughout the crystal as the atom is now ionized. The band theory can successfully explain non-integer values of magnetic moment per atom in the ferromagnetic materials. In genuine circumstances, neither one of the models can be deemed impeccably right, but instead a decent estimation. By a wide margin the best technique as of now accessible for figuring the magnetic properties of solids is Density Functional Theory (DFT), which incorporates every possible interactions between every electrons. This theory accepted that the electrons have the lowest energy configuration. Anyway, Density Functional Theory (DFT) measurements are so challenging because the correct type of interaction and the inter-electronic interaction energy is hard to find.

1.4.4 Antiferromagnetism

Antiferromagnetism is very similar to ferromagnetism. But the exchange integral (J_{ex}) in that case, have a negative value, which results in the anti-parallel orientation of the atomic magnetic moments and hence a net zero magnetic moment associated with the bulk material. In term of 'Heisenberg Hamiltonian interaction', the exchange energy is positive.

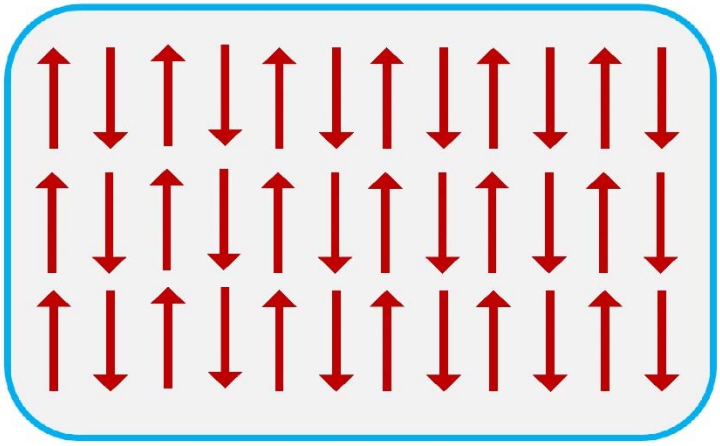

Fig. 1.15. Arrangement of individual magnetic moments in antiferromagnetic

The antiparallel ordering of the spins leads to produce very small positive susceptibility, as an applied field try to orient the spins which induced orientation is bigger than the diamagnetism of the orbital electrons. Like ferromagnetic materials, the exchange energy can be vanquished at higher temperature and hence the system moves toward becoming paramagnet.

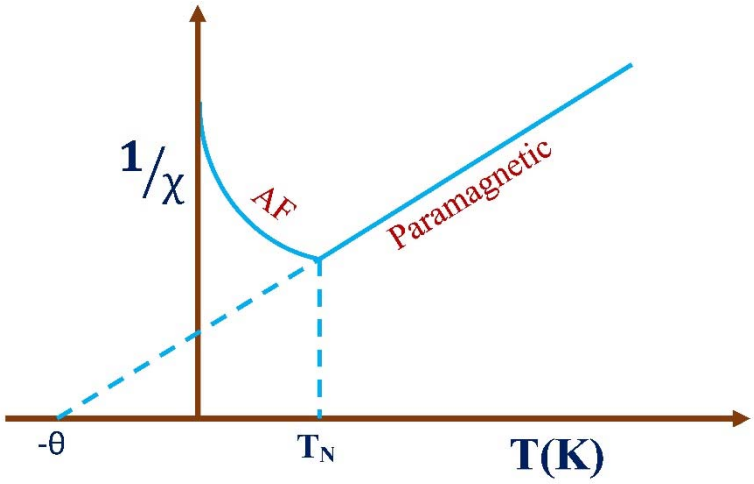

Fig. 1.16. Thermal variation of the reciprocal susceptibility of an antiferromagnetic material.

The dependence of the reciprocal susceptibility on the temperature of an antiferromagnetic material recorder to be minimum at a critical temperature known as Neel temperature (T_N). They have small positive susceptibility at all temperatures, though the susceptibilities changes in a peculiar way with temperature. The theory of antiferromagnetism was introduced by Neel [14]. When the temperature is below T_N, the susceptibility decreases due to the effect of thermal agitation which is responsible for the decrease of antiferromagnetic ordering of the moment. At higher temperatures the interaction effects is defeated by the thermal agitation and the susceptibility becomes analogous with that of paramagnet. If temperatures is higher than T_N, the antiferromagnetic susceptibility obeys the Curie -Weiss law along with a negative θ.

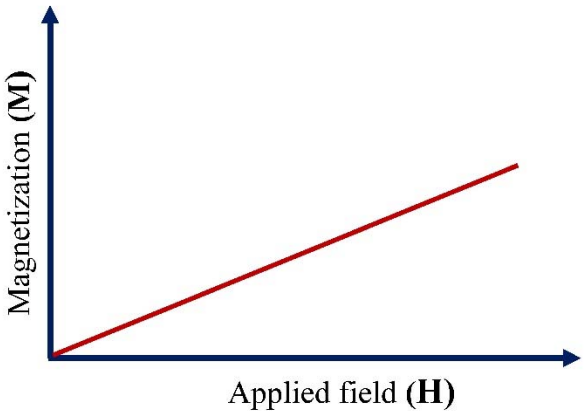

Fig. 1.17. M vs. H curve of antiferromagnetic substance.

An antiferromagnetic material can be seen infinitesimally comprising of two sub-lattice A and B and an antiparallel association happen between these lattices. These equivalent and inverse interaction remunerate each other in almost zero magnetization of

the antiferromagnetic material. Numerous antiferromagnetic systems are referred to, generally ionic compound, for example, metallic sulfides, oxides, chlorides and so forth.

According to Molecular Field Theory of antiferromagnetism, the resultant magnetization above Neel temperature associated with two sub-lattice can be written as

$$M = M_i + M_j = \frac{Ng^2\mu_B^2 s(s+1)}{3k_B T}\{H + (N_{ii} + N_{ij})M\} \qquad (1.28)$$

;where, N_{ii} and N_{ij} are the molecular field constants. Hence the susceptibility can be written in terms of paramagnetic Neel temperature (θ_N) as [15]

$$\chi = \frac{C}{T+\theta_N} \qquad (1.29)$$

Where, $C = \frac{Ng^2\mu_B^2 s(s+1)}{3k_B}$ and $\theta_N = -\frac{C}{2}(N_{ii} + N_{ij})$.

1.4.5 Ferrimagnetism

Like anti-ferromagnetic materials, the ferrimagnetic materials also consists of two sub-lattices, with atomic magnetic moments in anti-parallel directions but the atomic magnetic moments in the two sub-lattices are not equal to each other. So they cannot cancel each other and hence there is a net magnetic moment associated with the ferrimagnetic materials.

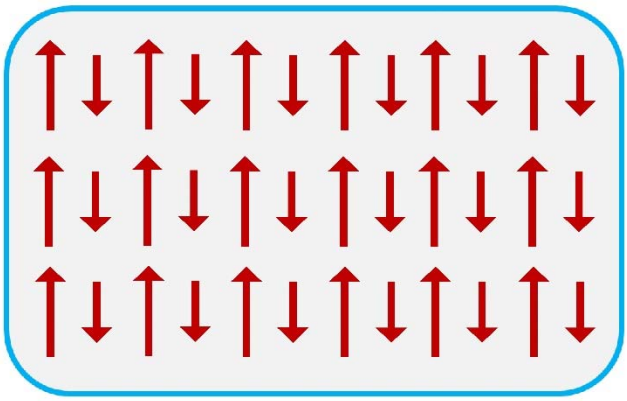

Fig. 1.18. Arrangement of atomic magnetic moments in ferrimagnetic materials.

Ferrimagnetism is also called as uncompensated antiferromagnetism. Like ferromagnetic materials, ferrimagnetic materials have a spontaneous magnetization below the critical temperature which is known as Curie temperature. Although the magnetic alignment of both ferromagnet and ferrimagnet is remarkably different but the magnitude of magnetic susceptibility for both material is similar.

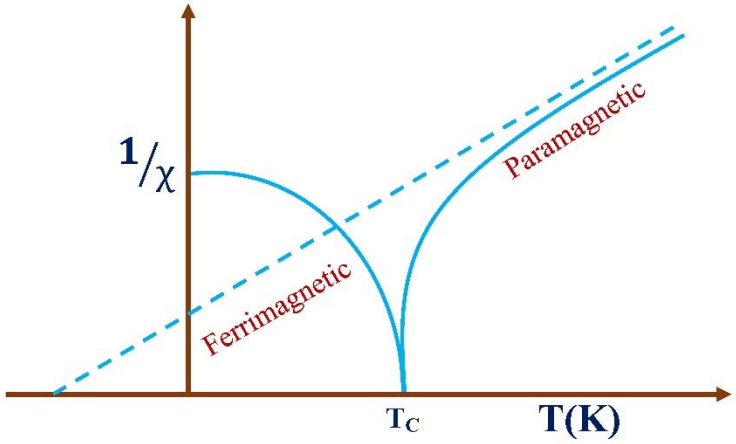

Fig. 1.19. Temperature dependent inverse susceptibility curve of ferrimagnetic substance.

The magnetic moments in ferromagnetic materials are divided into two sub-lattices and they are classified into a subset of antiferromagnetic materials. The major difference between ferrimagnetic and antiferromagnetic is that either the magnitude or number of moments of the two sub- lattices are different. The most versatile ferrimagnetic materials are iron double oxides as in $MOFe_2O_3$, where M stands for divalent metal. There are numerous ferrimagnetic systems are known: ferrites are a noteworthy class. Ferrimagnetism in ferrites in view of Neel's sublattice demonstrate are managed in detail in the following sections.

1.4.6 Superparamagnetism

An exclusive class of magnetic materials are superparamagnetic materials. They have only one domain and below Curie temperature (T_C) they are ferromagnetic in nature. When the temperature is above T_C, these superparamagnetic materials act as paramagnetic materials and they don't show any hysteresis. The concept of superparamagnetism was originally developed and proposed by Neel [16, 17] to explain the possibility of thermal fluctuations in single domain ferromagnetic clusters. If a particle of single domain turn out to be small enough so that the magnetic anisotropy energy KV (;where K depicts the magnetic anisotropy constant and V represents the particle volume) would become sufficiently small that the fluctuation of thermal energy could compensate the forces of anisotropy. As a result, the direction of magnetization changed from one easy direction to other even if there is no field. Because of the opposition between thermal energies and anisotropy, gathering up of small particles show behavior similar as like as paramagnetic materials, however with considerably larger magnetic moment [15]. The origin of moment is the moment associated with particle and related as $m=M_S V$. It may be very large and around a thousand Bohr Magnetons. An external magnetic field might try to orient this huge moment, but $k_B T$ will fight against the allignment similarly as on account of paramagnet. This phenomenon illustrate the superparamagnetism [8].

If the magnetic anisotropy become zero or very small then one ought to expect that the net moment could point in any possible direction. Henceforth Langevin Function can

be utilized to characterize magnetization $M = NmL(x)$ where $L(x) = Coth(x) - \frac{1}{x}$ as depicted in equation 1.14 and 1.15.in paramagnetism.

The two unmistakable highlights for superparamagnetic systems are (i) when the variation M is plotted against H/T, the magnetization curves for different temperatures will superimpose. (ii) The hysteresis is zero, i.e., both the remanence and the coercivity will be null. A typical hyteresis curve of superparamagneticmaterial is illustrated in Fig. 1.20.

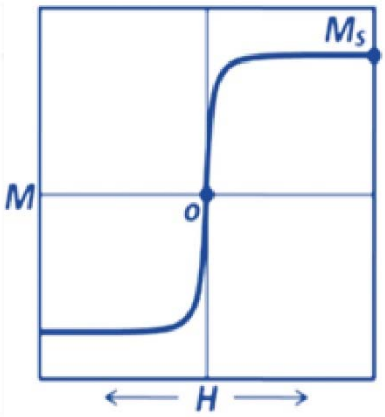

Fig. 1.20. Hysteresis curve of a superparamagnetic substance.

The anisotropy energy KV describes a barrier for the total spin re-alignment. Hence the jumping probability is proportional to the Boltzmann factor $exp(-\frac{KV}{k_BT})$. The moments of the particles can vacillate quickly at high temperature,. The relaxation time t of the particle moment can be represented as

$$\tau = \tau_0 \, exp(\frac{KV}{k_BT}) \qquad (1.30)$$

;where τ_0 is typically 10^{-9} s.

These changes drop-off (τ increases) when the sample is cooled and the system seems static when τ turns out to be considerably bigger than the estimating time of the appropriate experimental technique in laboratory.

The normal experiment with a magnetometer need 10 to 100 seconds using $\tau =$ 100 s and $\tau_0 = 10^{-9}$ s, we may acquire the critical volume as

$$V_{sp} = \frac{25k_BT}{K} \qquad (1.31)$$

A particle have a volume less than critical volume will behave like a superparamagnet on the 100s experimental time scale. The relation can be adjusted to yield

$$T_B = \frac{KV}{25k_B} \qquad (1.32)$$

;where T_B is known as blocking temperature. Below blocking temperature, the anisotropy will hinder the free mobility of the magnetic moment. Above T_B the system will be superparamagnetic.

1.5 Magnetic Anisotropy

The dependency of magnetic behavior on the direction through which they are studied, generally refers to magnetic anisotropy. Magnetic properties like magnetization and hysteresis of a magnetic materials is influenced by the type and magnitude of magnetic anisotropy. The critical and basic causes of anisotropy are magneto crystalline anisotropy, shape anisotropy, surface anisotropy and induced magnetic anisotropy, which will be discussed in proceeding sections [18].

1.5.1 Magneto Crystalline Anisotropy

The magneto crystalline anisotropy is most significant type of anisotropy. This type of anisotropy originate from the spin orbit interaction of the orbital electrons. The electron orbitals are linked to the crystallographic structure. The spins prefer to align themselves along a precise crystallographic axes as a result their interactions with orbital. Therefore, there are some directions in which a magnetic material can easily be magnetized. This directions are called the easy axes of magnetization for a magnetic material [19]. For example, the Iron (Fe) with bcc structure have the easy axis along the (100) plane, in fcc structured nickel the easy is axis is along (111) plane. It is interesting to notice that the saturation magnetization will be the same, i.e., the axis of magnetization does affects the value of saturation magnetization. But the field is acutely distinct in every cases to acquire that value of magnetization.

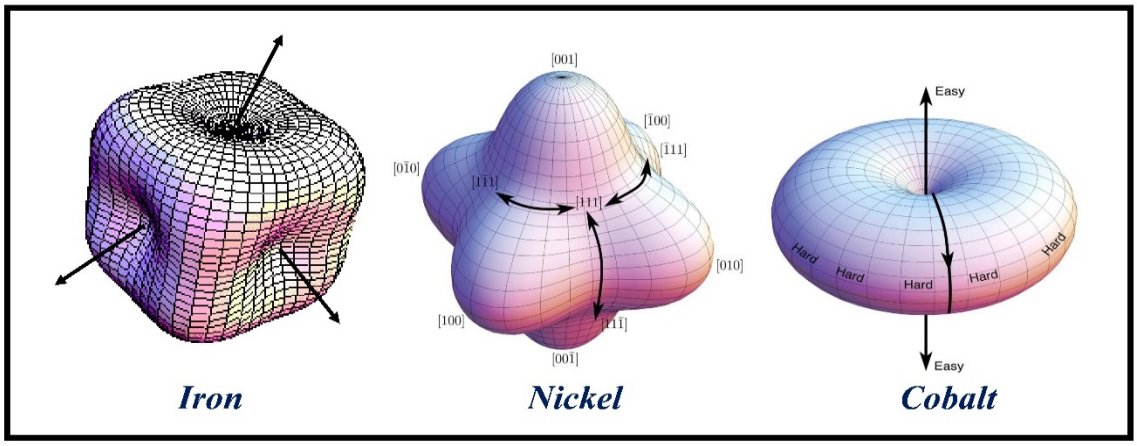

Fig. 1.21. Magneto crystalline anisotropy of Iron, Nickel and Cobalt.

The spin-orbit interaction can be evaluated from basic principles. However, we can use the phenomenological expressions in which the effect of crystal symmetry is taken into account and take the coefficients from experiment [19].

Orientation of the spins in other directions rather than the easy axes direction is govern by the increment of the anisotropy energy E_k. For a cubic crystal E_k depends on two anisotropy constants $K_1$and K_2 by the following equation

$$E_k = K_1(\alpha_1^2\alpha_2^2 + \alpha_2^2\alpha_3^2 + \alpha_3^2\alpha_1^2) + K_2\alpha_1^2\alpha_2^2\alpha_3^2 \qquad (1.33)$$

where, α_1, α_2 and α_3 are the direction cosines corresponds to the magnetization vector. In magnetic materials the anisotropy energy decreases as the temperature increases and near T_C, there is no precise direction for the magnetization of domain.

Table 1.1: Values of magneto-crystalline anisotropy constant (K_1) of some ferrites at room temperature.

Ferrite	Value of K1 in erg/cm3
Fe_3O_4	-1.1×10^3
$Co_{0.8}Fe_{2.2}O_4$	$+3.9\times10^6$
$Co_{1.1}Fe_{1.9}O_4$	$+1.8\times10^6$
$Co_{0.3}Zn_{0.2}Fe_{2.2}O_4$	$+1.5\times10^6$
$Co_{0.3}Mn_{0.4}Fe_2O_4$	$+1.1\times10^6$
$Mn_{0.45}Zn_{0.55}Fe_2O_4$	-3.8×10^3
$MnFe_2O_4$	-28×10^3
$Ni_{0.8}Fe_{2.2}O_4$	-39×10^3
$NiFe_2O_4$	-63×10^3

1.5.2 Shape Anisotropy

Polycrystalline material don't have any magneto crystalline anisotropy if the grain of the material doesn't have any precise direction of magnetization. But, if we consider the isotropic properties of the material then a particular energy is required to magnetize the material along any arbitrary direction is only given if the sample is spherical. If the sample is not spherical then at least one particular axis appear which illustrate the easy axes of magnetization and these are completely depends on the shape of the sample. This is the cause of shape anisotropy. The magneto-static energy density can be written as

$$E = \frac{1}{2}\mu_0 N_d M^2 \qquad (1.34)$$

where N_d is the tensor which depicts the demagnetized factor (measured from the proportion of the axis). M measures the saturation magnetization of a given sample. For instance the shape anisotropy energy of an ellipsoid which is uniformly magnetized is

$$E = \frac{1}{2}\mu_0 V(N_x M_x^2 + N_y M_y^2 + N_z M_z^2) \qquad (1.35)$$

where the tensor fulfilled the relation $N_x + N_y + N_z = 1$.

1.5.3 Surface Anisotropy

The main origin of the anisotropy in a small magnetic nanoparticles come from surface effects. When the crystal symmetry breaks in a sample then there is a decrease in nearest neighbors and the surface anisotropy appears. The defensive shell or ligand atoms which cover the small particles assume an imperative part also prompting a difference in the electronic condition on the particle surface.

1.5.4 Induced Magnetic Anisotropy

Induced magnetic anisotropy isn't inalienable to the material, yet it is delivered by treatment, for example, annealing and so on which has directional attributes. The easy axis and the magnitude of the anisotropy can be changed by applying the proper treatments. To produce this anisotropy in polycrystalline alloys one should use some methods, for example casting, rolling and wire drawing etc.

1.6 Magnetic Exchange Interactions

Exchange interaction is an essential phenomenon which administered the long range magnetic ordering in various magnetic materials. It is electrostatic in nature and have quantum mechanical origin. It is very effective, but acts between neighboring spin only and decreases drastically with seperation. Heisenberg illustrated the interaction between two atoms with spins S; in equation 1.27. There are different types of exchange interactions like direct exchange, indirect exchange or superexchange, RKKY interaction and double exchange etc.

1.6.1 Direct Exchange Interaction

In this type of exchange interactions, the interaction appeared between the neighboring spin which are acts directly and there is no other intermediary. Since the direct overlap between the neighboring orbitals are insufficient, hence the direct exchange doesn’t play an essential part to control the magnetic properties. Therefore direct interactions doesn’t affect the properties of rare earth and transition metals.

1.6.2 Indirect or Superexchange Interaction

In the case of ionic solid, there is an interaction between the non-neighboring magnetics ions which is intervened by a non-magnetic ion, kept within the magnetic ions. This type of exchange is called indirect exchange or superexchange interactions.

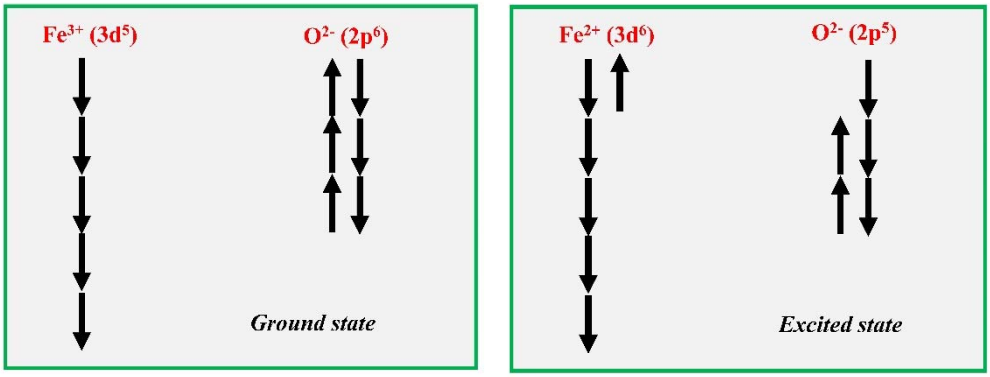

Fig. 1.22. Electronic spin distribution in super exchange interaction.

In ferrite, superexchange interactions is associated by the oxygen orbitals along with the metal atom. This process is second order which is deduced from the second order perturbation theory. Superexchange interactions could happen in ferromagnetic materials yet less normal than the typical antiferromagnetic or ferromagnetic superexchange.

1.6.3 RKKY Exchange Interaction

In metals, the conduction electrons are responsible for the exchange interactions between magnetic ions. The conduction electrons is polarized due to localized spin magnetic moment polarization and this leads to couple the polarization with a neighboring localized magnetic moment at a distance 'r'. The interaction is known as RKKY interaction after the name of Ruderman, Kittel, Kasuya and Yosida. This association is long range and it has a periodic reliance on the distance between the magnetic ions. The final interaction

might be ferro or antiferromagnetic which completely relies upon the distance between the magnetic ions.

1.6.4 Double Exchange Interaction

In a few oxides, it is conceivable to have a ferromagnetic exchange interaction which happens between the magnetic ions demonstrating a mixed state of valency. The ferromagnetic arrangement is by the reason of the double exchange mechanism. Zener proposed this exchange mechanism on the basis of the interaction between adjoining ions of parallel spins through a neighboring oxygen ion. Zener's process of double exchange creates a positive interaction which is leading aspect to the noticed ferromagnetic interaction in compounds such as perovskite manganates as $LaMnO_3$, $LaSrMnO_3$ etc.

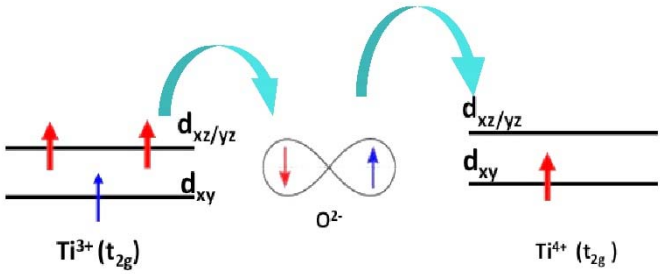

Fig. 1.23. Electronic spin distribution in double exchange interaction.

1.6.5 Anisotropic Exchange Interaction

It has been noticed that spin orbit interaction results in exchange interactions in the same way to that of the oxygen ion in superexchange. There is an exchange interaction occur between the excited state and the ground state of different ion. Here the spin-orbit interaction of a magnetic ion is responsible to produce the excited state. This is called the anisotropic exchange interaction or the DZyaloshinsky-Moriya interaction. The manner of the interaction is with the end goal that it attempts to constrain the spins to be at right angles

to the plane, so that the arrangement will affirm the energy is negative. The canting of spin by a small angle is the effect of anisotropic exchange interaction. The effect is called weak ferromagnetism. Its examples are α-Fe_20_3, $MnCO_2$ etc.

1.7 Ferrimagnetic Materials or Ferrites

Ferrimagnetic materials, i.e., Ferrites are a type of magnetic ceramics which contain iron oxide as a most important ingredient in it. It is now seven decades since the ferrites debuted as an extensive class of magnetic materials. These are now very well established group of magnetic materials. In present day ferrites have wide range of applications in modern technology, and have made their vast contribution in advance electronics. In this era of material science, ferrites having high relative permeability (up to 30,000) and power ferrites with high frequencies (up to 10 MHz) commercially available in the market. Despite the fact that, advancement and innovations keep on taking spot; numerous new applications, theories and synthesis methods are as of now a work in progress in field of ferrites.

Ferrite exhibits ferrimagnetisms which arises as a result of the super-exchange interaction among electrons of metal ions and oxygen ions present in the crystal. In ferrite, there is an antiparallel alignment of electronic spin with unequal magnitude. Hence the opposite spins are trying to lowering the magnetization compared to ferromagnetic metals. Due to this intrinsic atomic interaction in ferrite between metal and oxygen ions, it possess higher resistivity contrasted with ferromagnetic materials. This property empowers to find applications at higher frequencies and make it innovatively astounding. The magnetite

(Fe_3O_4) was the earliest natural occurring ferrite. Mixed metal oxides with iron(III) oxides as their primary constituent are known as ferrites. The research in ferrites was initiated by Kato & Takei (1933) [20], Kawai (1934) [21] and Snoek (1936) [22]. The initiation in preparation and development of ferrites was laid by Snoek [23] in 1946. The pioneering work of Snoek and the basic theory of ferrimagnetisms developed by Neel [24] were the starting point for rapid expansion of research activity in the field of ferrites. The first modern ferrite was prepared in 1946 [25]. In 1952 Hogan [26] made first workable ferrite based microwave generator. The other important characteristics of these materials are that they also possess good magnetic properties [27].

1.8 Classification of Ferrite

Ferrites can be categorize based on

(A) The value of magnetic coercivity.

(B) Crystal Structure.

(A) Classification of Ferrite: Based on Magnetic Coercivity

Concerning their magnetic properties, the ferrites are categorize as "soft" or "hard", which specify their low or high value of magnetic coercivity.

(i) Soft Ferrite

Ferrites are vastly utilized as cores in transformer and electromagnets which contain nickel, zinc, and/or manganese compounds, fall in the class of soft ferrites. The soft ferrite have a small value of magnetic coercivity. The low coercivity refers to the change in the

direction of magnetization at a cost of small amount of energy (hysteresis losses). Whereas the high resistivity of the material prevent the source of energy loss, like eddy current in the core. Due to these fascinating properties, like low loss at high frequency etc. they are widely used as inductor core and RF transformers in applications such as switched-mode power supplies.

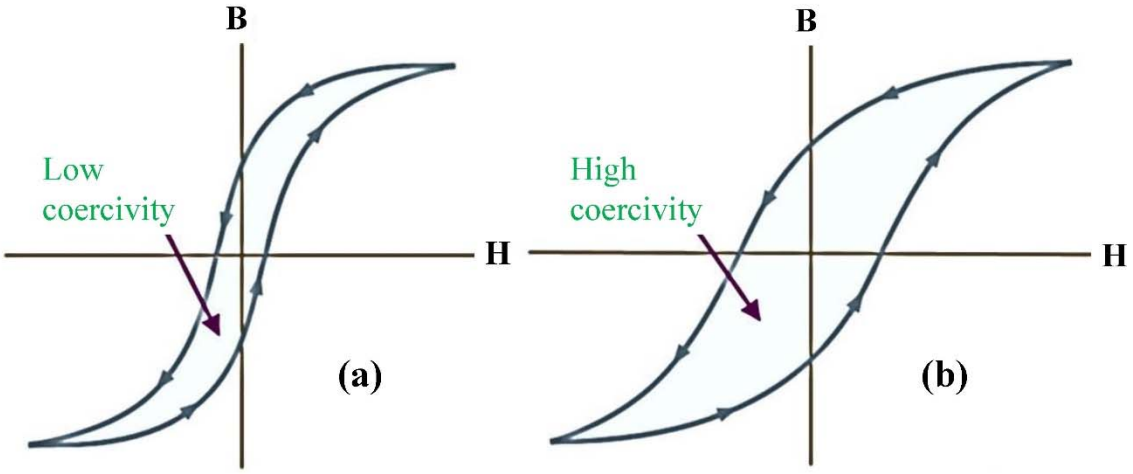

Fig. 1.24. Typical hysteresis loop of (a) soft ferrite and (b) hard ferrite.

(ii) Hard Ferrite

As opposed to the soft ferrites, hard ferrite have high magnetic coercivity and remanance. They are often used to build up permanent ferrite magnets. Mainly, iron and barium or strontium oxides are used as raw materials to synthesize the hard ferrite. The high coercivity implies that the demagnetization of the material is very, which is a fundamental aspect for a permanent magnet. Again they have high relative permeability and the conduction of magnetic flux is very good in the material. This properties of the ceramic magnet enable to store larger magnetic fields than iron itself. The production cost

of these materials are cheap so they are widely used in different household applications. Some experimental data suggest that the maximum magnetic field B ~ 0.35 tesla and the magnetic field strength H ~30-160 kA-turns/m (400 to 2000 Oe). The density is about 5g/cm^3. Ferrite cores are often used in electronic transformers, inductors and electromagnets due to very low eddy current loss which is governed by the high resistance of the ferrite. In present day a lump is seen in a computer cable, which are known as ferrite bead. It helps to protect the device from high frequency electrical noise (radio frequency interference).

(B) Classification of Ferrite: Based on crystal structure

In terms of the crystal structure, the ferrites are for the most part characterized into following four general classes:

(i) Spinel Ferrite

Spinel ferrites have spinel structure in crystal. This is named after the mineral spinel, having chemical formula $MgAl_2O_4$. The spinel structure is predominantly controlled by the oxygen ion lattice. The oxygen ions are occupied in *fcc* crystal arrangement in such way that there are two types of space between the anions which are tetrahedral A sites and octahedral B sites. The general formula of spinel is $M.Fe_2O_4$, where M denotes the divalent metal ions. The unit cell of ferrite consists eight formula units, i.e., total 56 ions contain in a unit

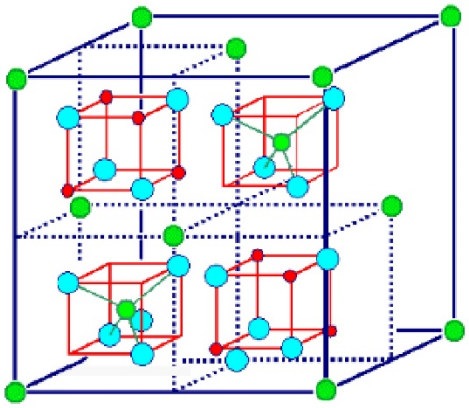

Fig. 1.25. Unit cell structure of a spinel.

cell. Thus there are 32 oxygen ions in a unit cell. There are total 64 tetrahedral lattice sites and 32 octahedral lattice sites. Only 8 lattice sites are angaged out of 64 tetrahedral sites, while 16 lattice sites are engaged out of 32 octahedral sites.

(ii) Garnet

Garnet ferrites named after the structure of the silicate mineral garnet which have the general chemical formula $M_3(Fe_5O_{12})$, where M is Yttrium or any rare-earth ion. In contrast with the spinel ferrite, the garnet have dodecahedral sites with tetrahedral and octahedral sites. Therefore the net ferrimagnetism is difficult calculate and one have to take account all antiparallel spin arrangement in three kinds of sites. Also the Garnets are hard magnet. The doping of different rare earth ion in ideal mineral garnet $Mn_3Al_2Si_3O_{12}$ was reported by Yoder and Keith in 1951. They have synthesized the first rare earth doped garnet $Y_3Al_5O_{12}$, which was silicon free by doping $Y^{III}+Al^{III}$ for $Mn^{II}+Si^{IV}$. In 1956 Bertaut and Forrat have measured the magnetic properties of $Y_3Fe_5O_{12}$. In 1957 Geller and Gilleo synthesized and studied the different properties of $Gd_3Fe_5O_{12}$ in 1957. The unit cell of an iron garnet consists eight formula units, which have the general formula $M_3Fe_5O_{12}$, where M indicates the trivalent rare earth elements, like Y, Gd, Dy ions. They have cubic cell with edge length is ~12.5 Å.

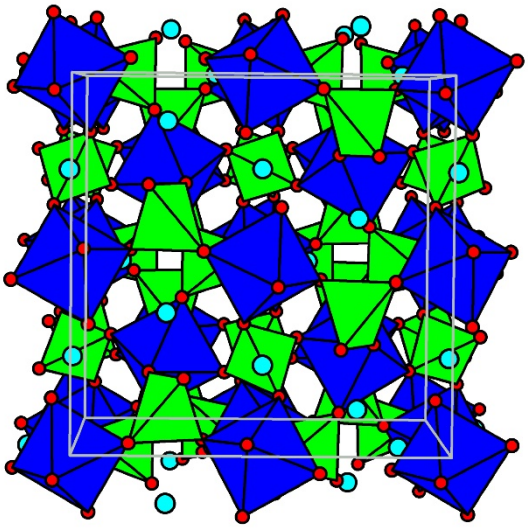

Fig. 1.26. Typical structure of a garnet.

(iii)Hexagonal Ferrite

The general chemical formula of hexagonal ferrites is $M(Fe_{12}O_{19})$, where M generally denotes Barium (Ba), Strontium (Sr) or Lead (Pb). The crystal structure in this type of ferrite is complicated. The crystal structure can be presented by a hexagonal closed packed structure with a unique vertical axis or c axis. This vertical axis in the crystal acts as the easy axis of magnetization. The hexagonal ferrites performed as hard ferrite, since the change of direction of magnetization along another axis is so difficult. This sort of ferrite was first perceive by Went, Rathenau, Gorter and Van Oostershout in 1952 and in 1956 Jonker, Wijn and Braun also reported the same. Oxygen ions are in the closed packed hexagonal crystal structure in these ferrites. Due to the large value of magnetic coercivity, these ferrites are extensively used as permanent magnets and also in high frequency applications. The lattice in the crystal structure of hexagonal ferrite is like that in the spinel structure, in which the oxygen ions closely packed. But in this case, there also metal ions occupy some layers, having same radii as of the oxygen ions in the crystal. In contrast to the garnet ferrite, hexagonal ferrites have larger ions which are produced by the substitution of oxygen ions. These bigger ions are mostly strontium, lead or barium [28, 29].

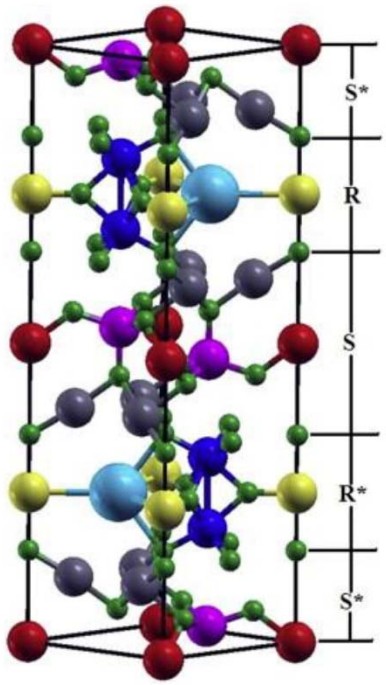

Fig. 1.27. Unit cell structure of a hexagonal ferrite.

Table 1.2: Different types of ferrites and their examples.

Type of ferrite	Structure	General formula	Examples
Spinel	Cubic	MFe_2O_4	M=Mn, Co, Ni, Zn, Mg, Cu, Li
Garnet	Cubic	$Ln_3Fe_3O_{12}$	Ln=Y, Sm, Tb, Eu, Dy, Gd, Tm, Er, Ho
Magnetoplumbite	Hexagonal	$MFe_{12}O_{19}$	Ba, Sr
Ortho	Perovskite	$LnFeO_3$	Ln= same as garnet.

(iv) Ortho Ferrite

The general formula of ortho ferrites is $MFeO_3$ where M is a giant trivalent metal cations such as Yttrium or rare earth ions. An orthorhombic unit cell in a distorted perovskite structure describes the crystal structure of this kind of ferrite. Weak ferromagnetism is found in this types of ferrites. The examples of these types of ferrites are $HoFeO_3$ and $ErFeO_3$ [30]. An orthorhombic distorted perovskite structure is found in the rare earth ortho-ferrites. The examples of this kind of ferrite $La^{3+}Mn^{3+}O_3^{2-}$ etc.

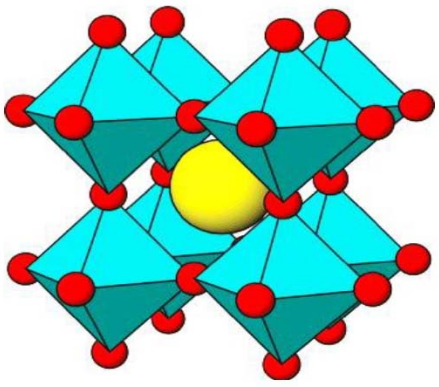

Fig. 1.28. Typical structure of an ortho ferrite.

1.9 Structure and Chemistry of Spinel Ferrite

Spinel ferrites have spinel structure in crystal. This is named due to similarity in the crystal structure of mineral spinel, having general chemical formula $MgAl_2O_4$. The spinel structure is especially described by the position oxygen ion lattice. There are two sorts of interstices between the components of such a lattice, tetrahedral interstices (A-site) having four nearest neighbors and the octahedral interstices (B-site) having six nearest neighbors. On the off chance that the tetrahedral sites are vacant and only the octahedral sites are occupied then the crystal is having the rock salt structure. Again if all the octahedral sites are empty and all the tetrahedral sites are filled, the crystal is having the zinc-blende structure. In spinel ferrites there are cations in both interstice. The occupancy of cations in octahedral site is twice the occupancy in tetrahedral sites. The spinel lattice might be expressed as an controlled mixture of the rock-salt and zinc-blende structure [31]. Cubic unit cell of spinel compounds contains eight smaller cubes called octants or formula units, corresponding to the formula of $A_8B_{16}O_{32}$. In 1915 Bragg and Nishikava [32, 33] were first to determine the spinel structure. The oxygen anions create a face centered cubic (*fcc*) close pack in which the cations are partially occupy both the tetrahedral and octahedral sites. The interstitial is at the center of a tetrahedron in A-site which is formed by four oxygen atoms. Three oxygen ions in a single plane are in contact with each other; the fourth oxygen ion placed in the symmetrical position on the top center of the plane containing three anions.

The cations are at the void formed by oxygen ions. In B-site of the spinel, six oxygen ions create an octahedron and the interstitial is situated at its center. Four anions are in contact with each other, the other two anions occupy the symmetrical position up and down to the center of the plane produced by four oxygen ions. Metal ion occupies the space formed by six oxygen ions creating an octahedral structure. The interstices in an ideal spinel structure of oxygen ions can incorporate only those metal ions whose ionic radius $r_{tetra} \leq 0.30$ Å in tetrahedral sites and those ions with ionic radius $r_{octa} \leq 0.55$Å in octahedral sites [34].

Table 1.3: Ionic radii of different cations in spinel ferrite.

Metal ions	*Ionic radius in Å*
Mg^{2+}	*0.78*
Mn^{3+}	*0.70*
Mn^{2+}	*0.91*
Fe^{2+}	*0.83*
Fe^{3+}	*0.67*
Co^{2+}	*0.82*
Ni^{2+}	*0.78*
Cu^{2+}	*0.70*
Zn^{2+}	*0.82*
Cd^{2+}	*1.03*
Al^{3+}	*0.57*
Cr^{3+}	*0.64*

In order to accommodate a wide variety of metal ions with ionic radii in the range from 0.40 Å to 0.90 Å the lattice has to undergo adjustment. Hence, the existence of ideal face centered cubic spinel structure quite impossible and the oxygen ions in the spinel are not normally occupy the correct location in the *fcc* sub-lattice. The oxygen ions govern the existance of cations in fcc spinel lattice. They form a three dimensional perforated enclosure for metallic cations exhibit in tetrahedral and octahedral sites; thereby imposing a cloud of restrictive dominance over metallic behavior of cations. The oxygen ions affect the electrical and magnetic behavior of spinel ferrites, since the cations are not independent here [35]. The ionic radii of various cations at A and B sites of the spinel structure are given in table 1.3.

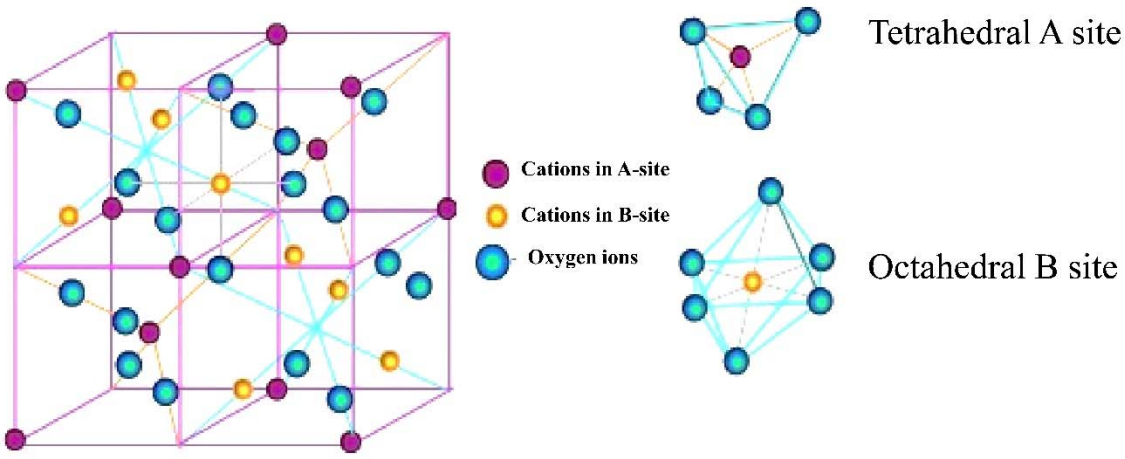

Fig. 1.29. Basic structure of a typical spinel ferrite.

The general chemical formula of spinel ferrites is $Me_{\delta}^{2+}Fe_{1-\delta}^{3+}\{Me_{1-\delta}^{2+}Fe_{1+\delta}^{3+}\}O_4^{2-}$. Octahedral sites are represented by square brackets and the cations prior to square brackets are that of tetrahedral sites. Here, δ is degree of inversion which determines the classification of ferrites. Depending on the distribution of different cations at different

crystallographic positions, the compounds of spinel can generally be classified into following categories [36].

(A) Normal Spinel: δ=1

(B) Inverse Spinel: δ=0

(C) Mixed Spinel: 0 < δ < 1

(A) Normal Spinel

In normal spinel ferrites all Me^{2+} ions occupy tetrahedral sites, i.e., 8 tetrahedral sites are possessed by 8 bivalent cations and 16 octahedral sites are possessed by 16 trivalent cations. Structural formula of these ferrites is $Me^{2+}\{Fe_2^{3+}\}O_4^{2-}$. Zinc ferrites $ZnFe_2O_4$ have normal spinel structure. Fig. 1.30 illustrate the normal spinel structure.

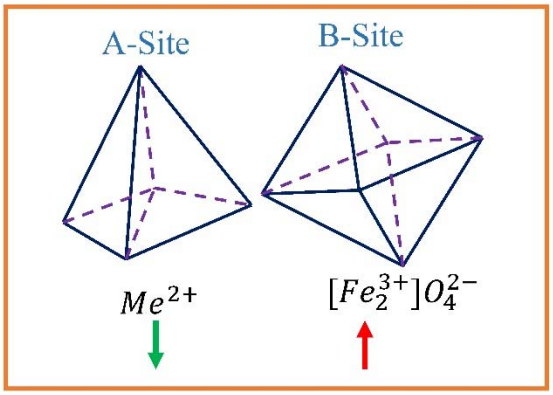

Fig. 1.30. Cation distribution in normal spinel ferrite.

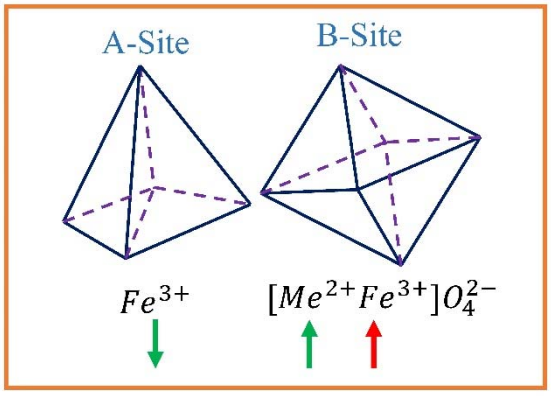

Fig. 1.31. Cation distribution in inverse spinel ferrite.

(B) Inverse Spinel

In inverse type spinel ferrites all the metal ions (Me^{2+}) are occupied by B-sites and Fe^{3+} ions are equally shared by tetrahedral (A) and octahedral (B) sites. The structural formula

of this kind of ferrites is $Fe^{3+}\{Me^{2+}Fe^{3+}\}O_4^{2+}$. Fe_3O_4, $NiFe_2O_4$ and $CoFe_2O_4$ are the example of inversed spinel structure. Fig. 1.31 illustrate the inverse spinel structure.

(C) Mixed Spinel

If the divalent metal ions (Me^{2+}) are available on both tetrahedral and octahedral sites then the ferrites is called mixed spinel ferrite. The structural formula for this kind of ferrite is $Me_{\delta}^{2+}Fe_{1-\delta}^{3+}\{Me_{1-\delta}^{2+}Fe_{1+\delta}^{3+}\}O_4^{2-}$. $MnFe_2O_4$ is an important example of this kind of structure and it has a degree of inversion δ = 0.2. Hence its structural formula become $Mn_{0.8}^{2+}Fe_{0.2}^{3+}\{Mn_{0.2}^{2+}Fe_{1.8}^{3+}\}O_4^{2-}$. Fig. 1.32 illustrate the mixed spinel structure.

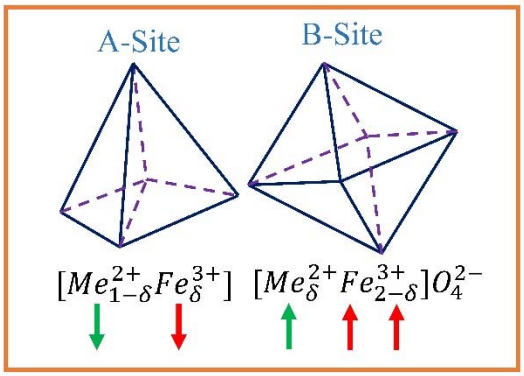

Fig. 1.32. Cation distribution in mixed spinel ferrite.

Spinel ferrite crystal related to the cubic structure with space group *Fd3m*. There are Z = 8 formula units in a unit cell that contains 32 O^{2-} ions in a face-centered cubic packing (*fcc*). Inside the spinel lattice which is formed by the anion, there are 32 octahedral and 64 tetrahedral interstices are available for cations. However only 24 of the total 96 interstices are occupied in a spinel lattice. In spinel A-site tetrahedra are isolated from each other however they share the corners with neighboring B-site octahedra. There is no edge sharing between the tetrahedral A-site and other polyhedral A- and B-site. Octahedral B-

site provide six of twelve O-O edges with nearest neighbour B-site octahedra. The other six edges are imparted to octahedra that encompass 16 empty sites. The O-O edges are shared by the B-site cations form a chains along the (110) direction. B-B distances are short on the grounds that no mediating anions impede neighboring B-site cations; this facilitates electrical conduction via hopping between B-sites [37].

The traditional choices for the origin of unit-cell in spinel ferrite can made in two ways, i.e., either on the A- site cation which have $\overline{4}3m$ symmetry or on the octahedral vacancy which have 3m symmetry. Anions are always belongs to the position 32e. The positions of the anions at the points 32e are not fixed, rather they vary depending on the anion positional parameter, *u*. For an exact *fcc* anion ordering, $u_{\overline{4}3m} = 3/8$ and $u_{3m} = 1/4$, respectively [38]. Anions in spinel normally depart from their exact *ccp* positions. This movement has various vital consequence, like changing in bond lengths and angles, modifications in interstice volumes and the coordinate symmetries in polyhedra [37]. Depending on the radii ratio of A/B, there are expansions or contractions of anion sub-lattice by relying *u*, until the volume of the A- and B- interstices voids match the radii of cations of constituent elements. As *u* increments from its original value, anions will move along the (111) direction away from the cations wich are tetrahedrally coordinated, which also increases the volume of each tetrahedral site, while volume of the octahedral sites become unchanged [38]. The symmetry of the regular tetrahedra corresponds to A-sites is unaltered by the anion-lattice extension. However, B-sites symmetry being reduced. This changes in symmetries of the site with anion dilations will affect the bond-angle variations with *u* [37].

1.10 Cation distribution in Spinel Ferrite

The physical and chemical behaviors of spinel ferrites are characterized by the sort and concentration of different cations integrated at tetrahedral and octahedral sites. The ferrite unit cell comprises of 56 molecules; 32 oxygen anions are disseminated in close-packed cubic structure and 24 cations possess 8 of the 64 tetrahedral sites and 16 of 32 octahedral sites accessible [39]. The oxygen atoms in ferrites are non-magnetic but play a very important role in regulating electrical and magnetic properties. Though the metallic ions at the interstices should ideally lay down the foundations for metallic behaviour, in reality it is not so due to the large separation between various cations, that makes cations non-interacting in the absence of any oxygen atoms. Oxygen ions facilitate the interaction by providing a connecting path for isolated cations. Since the spinel structure is very complex, and as a matter of fact the interaction of cations at interstitial sites and sub- lattices is also challenging. A wide variety of cations can occupy the interstitial sites so the knowledge of cation distribution is important criteria for understanding the origin of electrical and magnetic properties in spinel ferrite. The cation dispersion in a spinel ferrite depends on various factors, for example, synthesis method, ionic radii, ionic charge, calcination temperature, lattice energy, crystal field stabilization energy, octahedral site preference energy etc. [40].

The ideal tetrahedral site can incorporate a cation with maximum radius of 0.30 Å and octahedral site can accommodate a cation with maximum radius 0.55 Å. But since the transition metal ions such as Mg, Ni, Zn, Fe, Mn etc. have larger ionic radius than the ideal

volume available at these sites, the tetrahedral and octahedral sites undergo expansion in order to incorporate larger ions. Tetrahedral sites always undergo greater expansion as compared to octahedral sites. This further, forces oxygen ions to move outwards leading to increase in oxygen position parameter u [34]. Since cation distribution describe the foundations of magnetic and electrical properties of ferrites, its determination always enables a greater insight in to the atomic level interactions in the crystal.

1.11 Néel's Theory of Ferrimagnetism

Néel established his theory on the assumption that a ferromagnetic crystal can be separated into two sub-lattices formed by tetrahedral (A) and octahedral (B) sites in spinel structure. These sub-lattices have unequal and anti-parallel magnetic moment. This disparity of magnetic moments is attributed to [41]:

(1) Distinctive elements in various sites.
(2) Same elements in various ionic states.
(3) Non-uniform distribution of crystalline fields.

Neel's model further assumes that A and B sub-lattices have identical magnetic ions. Out of total number n of magnetic ions in unit volume, a fraction λ is situated at A-site and μ is on B sites. The possible interaction between the magnetic ions can be A-A, A- B, B-A and B-B. Furthermore A-B and B-A interactions are assumed identical. Let μ_A and μ_B are the average moments of a single ion, each at A-site and B-site in the external magnetic

field. Despite the fact that, the A- and B- sites ions are identical, $\mu_A \neq \mu_B$ because the cations in A- and B-site experience unequal fields.

Considering $M_A = n\mu_A$ and $M_B = n\mu_B$ and Weiss molecular field theory, that lays down the quantum mechanical foundation of ferrimagnetic material in exchange interaction between the ions located at various sites. The molecular fields acting on sub-lattice A and B are given as [41]:

$$H_A = \gamma_{AB}[\lambda\alpha M_A - (1-\lambda)M_B] \quad (1.36)$$

$$H_B = \gamma_{AB}[\beta(1-\lambda)M_B - \lambda M_A] \quad (1.37)$$

;where, $\alpha = \gamma_{AA}/\gamma_{AB}$, $\beta = \gamma_{BB}/\gamma_{AB}$ and γ_{AA}, γ_{BB}, γ_{AB} are Weiss constants.

These expressions lead to the equation for susceptibility for temperature above Curie temperature (T_C) [41].

$$\frac{1}{\chi} = \frac{T}{C} + \frac{1}{\chi_0} - \frac{\xi}{T-\theta} \quad (1.38)$$

;where, $C = {Ng^2\mu_B^2 J(J+1)}/{3k_B}$ (1.39)

$$\frac{1}{\chi_0} = \gamma_{AB}[2\lambda(1-\lambda) - \alpha\lambda^2 - \beta(1-\lambda)^2] \quad (1.40)$$

$$\xi = \gamma_{AB}^2 C\lambda(1-\lambda)[\lambda(1+\alpha) - (1-\lambda)(1+\beta)]^2 \quad (1.41)$$

and, $\theta = \gamma_{AB} C\lambda(1-\lambda)(2+\alpha+\beta)$ (1.42)

Upon inserting $1/\chi = 0$ in the above condition for Weiss constant, the Néel temperature is given by

$$T_N = \frac{\gamma_{AB}C}{2}[\alpha\lambda + \beta(1-\lambda) + \left\{(\alpha\lambda - \beta(1-\lambda))^2 + 4\lambda(1-\lambda)\right\}^{\frac{1}{2}}] \qquad (1.43)$$

Equation (1.43) represents a hyperbola as depict in Fig.1.33. The plot intersect the temperature axis at a temperature T_P which is known as Curie point.

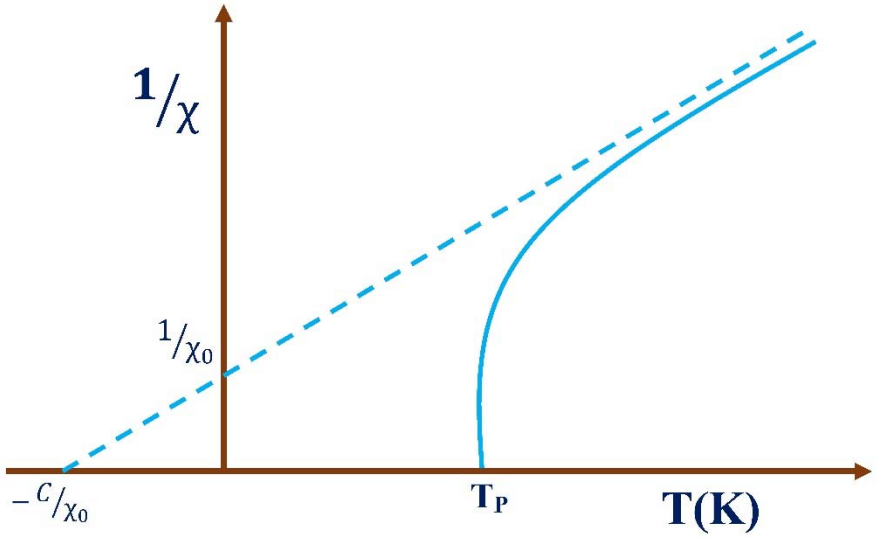

Fig. 1.33. Susceptibility variation with temperature according to Neel theory.

Metallic ions in spinel ferrites occupy two crystallographic different sites. Three kinds of magnetic interaction are conceivable between metallic ions located at octahedral and tetrahedral sites. This interaction is mediated by oxygen ions since the separation between cations is too large for any direct interaction. This interaction is characterized as superexchange interaction i.e. tetrahedral-tetrahedral (A-A) interaction, octahedral-octahedral (B-B) interaction and tetrahedral-octahedral (A-B) interaction.

The interaction energies are negative hence anti-parallel arrangement of spins of unpaired electron is induced. The amount of interaction energy between two magnetic ions, Me^{I} and Me^{II} depends on following two factors [42]:

(a) Distances between cations located at A and B sites and the intermediate oxygen atom.

(b) The angle Me^{I}-O- Me^{II} represented by the term ϕ as shown in Fig. 1.34.

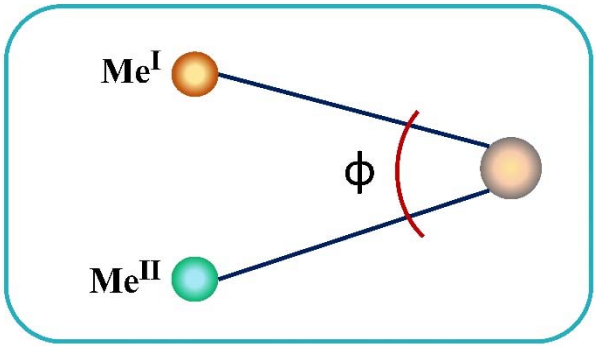

Fig. 1.34. Representation of Me^{I}-O- Me^{II} angle in spinel ferrite.

Interaction energy is maximum for $\phi = 180^{O}$ and decreases rapidly with distance. Fig. 1.35 represents various configurations of ion for magnetic interaction. A-B interaction have greatest magnitude compare to other possible interactions. Two conceivable arrangements for A- B interaction have little separations (p, q and p, r) and the estimations of ϕ are high. In the case of B-B interactions, only first arrangement is viable on the grounds that the separation s is too large for effective interaction. The A-A interaction is the m one because the separation r is too large and angle ϕ is 80^{O}.

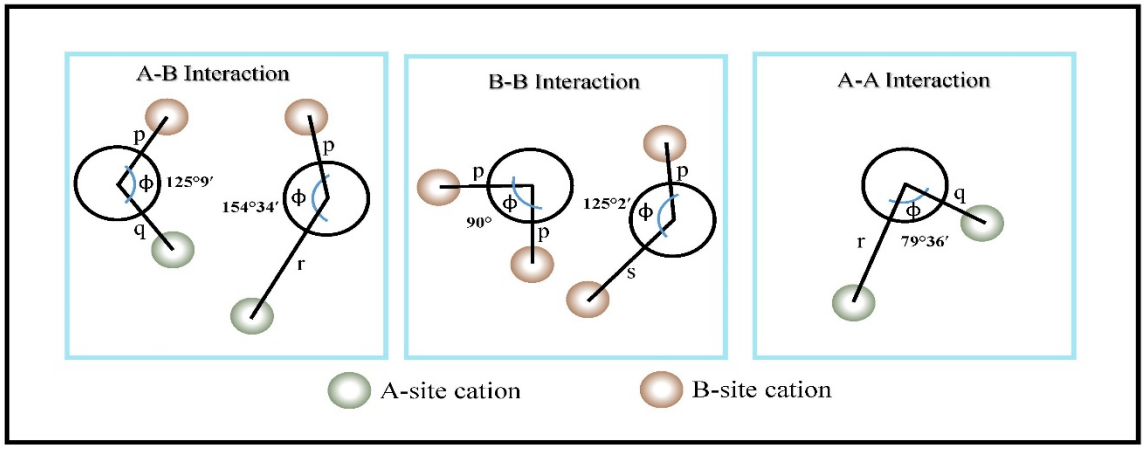

Fig. 1.35. Illustration of various possible configurations of ion pairs for effective magnetic interaction.

Thus A-B magnetic interaction is prominent and the spins of ions have antiparallel orientation at A and B sites. This ensures that the sub-lattice A and B are magnetized in opposite direction and the net magnetic moment is equivalent to the contrast between magnetic moments at A and B sites. Generally, magnetic moment at B sub-lattice (M_B) is greater than the A sub-lattice (M_A). The net magnetization can be expressed as [42].

$$M = |M_B - M_A| \qquad (1.44)$$

Table 1.4: Curie temperature (T_C) and saturation magnetization (M_S) of some ferrite.

Ferrite	Curie Temperature (T_C) in K	Saturation magnetization (Ms) in μ_B	
		Calculated	Observed
Fe_3O_4	858	4	4.1
$NiFe_2O_4$	858	2	2.3
$CoFe_2O_4$	793	3	3.7
$CuFe_2O_4$	728	1	1.3
$MnFe_2O_4$	573	5	4.6
$Li_{0.5}Fe_{2.5}O_4$	873	2.5	2.6
$ZnFe_2O_4$	9	0	0

Shortcomings of the Néel's model are [41]:

(a) Saturation magnetization esteems in various ferrites are observed to be much lower than those anticipated from Néel's model.

(b) Some magnetization versus temperature curves have limited slopes at 0 K and can't be clarified by Néel's model.

(c) It assumes that strong negative AB interaction prevails over A-A and B-B interactions, which isn't pertinent to every single case.

The Néel's model was failed to explain magnetic properties of complex ferrites because of assumptions which do not allow the natural fluctuations in superexchange interaction due to compositional variation [43]. More comprehensive explanation of magnetic properties could be obtained later by considering non-collinear spin structures (Yafet – Kittel arrangement) as described in the next section.

1.12 Yafet-Kittel Theory of Ferrimagnetism

There are a critical takeoffs from the Néel's collinear model shown by some ferrites with more than a few tenths non-magnetic substituent atoms per formula unit. Yafet and Kittel (1952) first expressed that the non-magnetic substitutions on one sub-lattice could induce a non-collinear or canted spin arrangement on the other sub-lattice. They recommended a split sub-lattice molecular field model to calculate a uniform canting angle θ_{YK} [44]. This sub-division was a departure from the collinear arrangement of spins assumed in Néel's model. Yafet and Kittel proposed a triangular type of spin structure in order to provide a more satisfactory theory of magnetism for spinel ferrites. When non-magnetic ions are substituted in spinel ferrite spin canting takes place which this gives rise to strong anti-ferromagnetic interaction among the B sites. This further divides the sub-

lattice into two sub-lattices of inclined spins corresponding to their inclination to be all the while anti-parallel to both A and B site neighbors.

The spin magnetic moments of B site cations will craete sub-lattices, in every one of which the moments are parallel. But moments in single sub-lattice is inclined and form an angle with the moments of another sub-lattice. This results in anti-parallel to A site moments. To account for the different magnetic ordering allowed by the crystal symmetry, A and B sub-lattices are additionally isolated into proportional sub-divisions. The A sites are splits into two sub-divisions while B sites into four sub-divisions. These four could be clubbed together to shape two non-proportionate sub-lattices.

A sub-lattice is separated into two (A′, A″) *fcc* lattices while the B lattice into four (B_1, B_2, B_3, B_4) *fcc* lattices, each having similar cube edge as in the spinel lattice. A site from A′ has four sites from A″ as closest neighbors in the A sub-lattice. A site from B_1 has six sites, two from the every one of the other three B_i, as the closest neighbors in the B sub-lattice. The interactions between any two B_i's are equal [45].

Accepting just a similar kind of magnetic ions exists, accordingly the Y-K treatment yields the accompanying outcomes.

$$H_A = n[1/\beta' - \alpha]M_A \qquad (1.45)$$

$$H_B = n[\beta' - \beta]M_B \qquad (1.46)$$

;where, α′β″=1, $\alpha' = \gamma_{AA'}/\gamma_{A'B}$ and $\beta' = \gamma_{BB'}/\gamma_{AB'}$

Finally, they have the Y-K angle as

$$sin\psi = \frac{1}{\beta'}\frac{M_A}{M_B} \qquad (1.47)$$

And this is possible when $\beta' < \frac{M_A}{M_B}$.

Thus the spin magnetic moments cannot be tilted in A and B sub-lattices at the same time. The estimations of M_A and M_B are temperature dependent, so that transitions between different arrangements might happen in the similar substance at various temperatures. It turns out consequently from the Y-K treatment (Fig. 1.36) that such transitions require not have a reason in temperature dependent interactions.

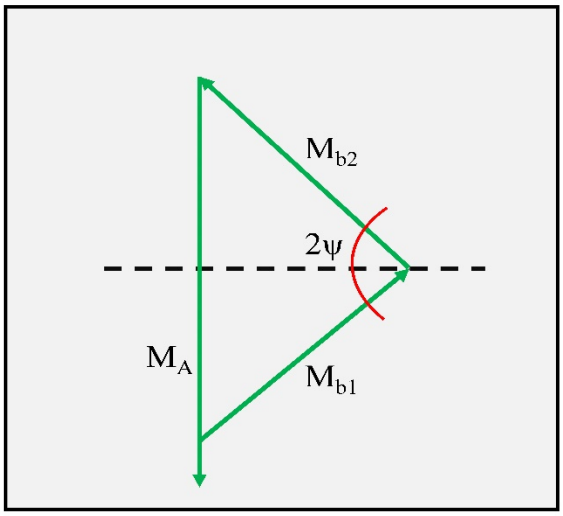

Fig. 1.36. Triangular spin configuration according to Y-K model.

The Yafet-Kittel model yields following equation for Y-K angles associated with the tilted magnetic moment.

$$n_B = M_B cos\psi_{YK} - M_A \qquad (1.48)$$

1.13 Application of Ferrite

Ferrite has been perceived as one of the most paramount electro-ceramics in modern technology. The handling and utilization of ferrite in innovation has been enhanced ceaselessly over the most recent two decades. From the 1950 as radio and TV spreads ferrites built up itself a noteworthy turning point in industries and now ferrite are most fundamental material in electronic industries [46].

Ferrites are used at both radio and microwave frequencies. There are various applications of ferrite below microwave frequencies. When ferrite rod is inserted into a coil of wire, will act as an antenna. It concentrates the electromagnetic energy in the core because of its high permeability. The combination of high resistivity and high permeability of ferrite also makes them a suitable filter in inductor applications. They also used as the cores of magnetic memories and switches. These applications involved the use of microsecond pulses for transmitting signals and reading information expressed in binary code. Other non-microwave applications are like IF amplifier transformer and tune inductors.

Ferrites are utilized at microwave frequencies for to some degree diverse reason. At these frequencies they display non reciprocal properties i.e. the attenuation and phase shift have distinctive quantities for microwave propagating through them in two opposite directions of propagation in a wave guide. A rather renowned Faraday Effect is observed at microwave frequencies i.e. the plane of polarization of the wave is rotated as it travels through an axially magnetized ferrite pencil in a circular wave-guide. This effect can be

used to build a whole kind of non-reciprocal devices such as unilines, gyrators and differential phase shifter etc. [47].

Recently, ferrites were considered as one of the most extensive magnetic materials to build up multilayer chip inductor (MLCI) and surface mount devices (SMDs) because of their high permeability and resistivity. The ferrite material system display super-paramagnetic behavior, small or zero remanence and coercivity and very high saturation magnetization induce them in potential applications such as magnetic drug delivery, biomedicine and cell sorting systems. Now ferrites are most important material in electronic industries. Ferrites are widely used magnetic materials due to some fascinating properties like high electrical resistivity, high permeability, low eddy current loss and dielectric losses, low cost of production etc. Furthermore nano ferrites have outstanding electric and magnetic properties which are comparably different from micro structured materials, fitting them to present day advances, as well as contributing novel applications, for example, magnetic drug delivery, high density information storage, ferrofluids, photo-catalysis, gas sensors, etc.

A few more applications of ferrites [47-49] are described below:

Inductors: Ferrites are fundamentally utilized as inductive segments in various electronic circuits such as filters, low noise amplifiers, impedance matching networks, voltage- controlled oscillators etc. Their present applications as inductors comply with the general pattern of scaling down and integration as ferrite multilayers for passive functional electronic devices. The multilayer innovation assume a basic part for large scale

manufacturing of integrated circuit. Multilayers help to make a high degree of integration. . Multilayer capacitors went to the market a couple of decades prior, while inductors began its voyage in the 1980s.

High Frequency Application: The demand of different magnetic materials has been increased in recent years for high-frequency applications, for example, radio, TV and tele-communications. The microwave technology needs very high frequencies and the bandwidth is up to100 GHz. Ferrites are non-conducting ceramic oxides as a result thus conversely with metals where the skin effect oppose the penetration of high-frequency fields, there is total penetration of E.M. fields in ferrites [48].

Power Application: Power supplies are required to operate almost all devices such as radio, TV, computers, all types of peripherals, video systems, audio systems and other small and medium instruments. The basic applications in the systems is called switched-mode power supplies (SMPS). In this type of application, first the primary power signal is rectified and then it switched to generate a regular high frequency rectangular pulses to feed into a ferrite transformer, and finally the signal is again rectified to supply the necessary power to the instrument. An expansion in power delivery and efficiency can be tuned by increasing the working frequency of the transformer.

Electromagnetic Interference (EMI) Suppression: In recent years there is a notable enhancement in the different kinds of electronic equipment, for example, computers, laptop, digital cameras, notebooks, scanners etc. in small areas. As a result the chances of disturbing each other due to presence of electromagnetic interference (EMI) has

been increased. Basically, the interference induced by electric and magnetic fields has enhanced due to vast development of wireless communications. Electromagnetic interference can be characterized as the degradation in performance of an electronic system due to an electromagnetic disturbance [50]. The electromagnetic noise in an electronic circuit is normally created at frequencies higher than the frequency of the circuit signals. To reduce or avoid the EMI, a suppressors is used to work as low-pass filters. It will block signals with higher frequencies than a particular frequency. There are so many way to construct an EMI suppressors: soft ferrites [51], ferromagnetic metals [52], ferromagnetic metal/hexaferrite composites [53], encapsulated magnetic particles [54], and carbon nano tube composites [55].

High-density optical recording: A defect spinel ferrite thin films can be used as write-once read-many optical recording system which work in blue wavelength region. Because of the meta-stable nature of these non-stoichiometric ferrites, they can be converted into corundum phases by a laser spot at moderate temperatures. The reconstructed regions have various optical indices from the starting ferrite film, make the readout process conceivable.

Magnetic sensors: These are utilized for temperature control and these can be made utilizing ferrite with sharp and specific Curie temperature. Position and rotational angle sensors (proximity switches) have likewise been designed utilizing ferrites.

Magnetic shielding: A radar absorbing ferrite paint has been invented. It is used in several military aircraft, ships and submarines for different stealth operation.

Pollution control: Recently, in Japan several ferrite based pollution control system have been installed. They are using the precipitation of ferrite precursors to scavenge the pollutant substances from waste materials. Subsequently produced ferrites are magnetically removed along with the pollutant.

Ferrite electrodes: Due to the existence of high corrosion resistance, ferrites having the proper conductivities have been utilized as electrode in applications, for example, chromium plating.

Entertainment ferrites: Ferrites have extensive application in radio, computer, audio-video system, television circuits. Ordinarily applications incorporate fly back transformers, deflection Yokes and SMPS transformer for power applications.

Copier Powders: copier is definitely not a magnetic recording instrument. But it is necessary to store the hard copies of the computer output. For this situation the main ascribe to the bearer powder in xerographic copiers is that it be magnetic. . Nonetheless, as of late, the carrier powder and the toner powder have been mixed into one material. Some magnetic oxide powders satisfy both requirement of carrier and toner powder and thus it very well may be utilized as a solitary powder material.

Radio and Television Antenna: The wavelengths related with radio and TV are relatively bigger. To correlate these wavelengths, the antenna should also be very large. Despite that, as magnetic materials have the capacity to focus the receiving signal or electromagnetic wave, in this manner antennae consists of magnetic material may be very small. This factor is particularly imperative in little portable radio or TV sets [47].

1.14 Literature Review

The journey of ferrite have been started probably six-seven decades ago, and continuing till the date. On present day, lots of researcher, scientist and students are investigating on different ferrite system to find out some interesting aspects which will develop the recent technology. Some factors which influence the properties of ferrites are the type and concentration of substitution, preparation technique, chemical composition, sintering temperature and different types of irradiation etc. Since the investigation on ferrites is so giant, subsequently it is so hard to gather all the test results and data about a wide range of ferrites in each perspective that is the reason confine ourselves to show an orderly survey of various hypothetical and test certainties identified with this present investigation. This literature survey not only highlights the various modifications attempted by various researchers and to mention the updated research activities in this important field but also to recognize the possible potential applications for which this material is of crucial significance.

The magneto-capacitance and dielectric properties of CZFO-PZT composite was investigated by Mandal *et al*. It was reported that the microwave assisted sintering procedure was used to develop the high quality multiferroic composite of CZFO-PZT, synthesized through sol-gel technique, which noticeably improve the dielectric and magnetic behavior of the composite. They showed that the dielectric loss decreases 1.2 times as compared to the conventional sintering technique [56].

Mandal *et al*. [57] investigated the magneto-electric response of CZFO-PZT multiferroic composite. They observed that the composite showed very good hysteresis loop with coercivity 83-124 Oe and spontaneous magnetization was about 20-24 emu/g. They also reported that the paraelectric to ferroelectric transition temperature was decreased with particle size. The optimal magneto-electric response was seen to be 0.6% for higher temperature sintered composite.

Kolekar *et al*. investigated the grain and grain boundary effects on the frequency and temperature dependence of dielectric properties of Co ferrite-Hafnium composite. It was reported that Hf induced a transition from grain dominated mechanism to grain boundary dominated mechanism of the dielectric relaxation in CFO [58].

The temperature and frequency dependent dielectric behavior of Zn doped Li-Mg ferrite was investigated by Shaikh *et al*. They showed that the change of dielectric constant and DC resistivity had opposite trend and concluded that the mechanism of dielectric polarization was same as the conduction process [59].

Dysprosium doped $Ni_{0.8}Co_{0.2}Fe_{2-x}Dy_xO_4$ ferrite was synthesized using simple ceramic method by Kadam et al [60]. All the samples showed common dielectric dispersion having Maxwell-Wagner type of interfacial polarization. The complex impedance studies confirm the existence of grain boundary contribution at low frequency. It was farther reported that the Dy doped Ni-Co ferrite is a semiconductor in nature.

Mandal *et al*. [61] synthesized Ni-Zn ferrite utilizing chemical pyrophoric reaction technique and investigated the dielectric and electrical properties. From the ac conductivity

data they concluded that the temperature activated electronic transport process has been attributed to large polaronic hopping in that system.

Gadolium doped cobalt ferrites had been synthesized using solid state reaction method by Rahman *et al.* The X-ray study affirmed the inverse spinel nature of the crystal structure. The frequency dependent dielectric study at room temperature obeyed the reshaped Debye equation. The dielectric constant was enhanced due to Gd doping. The activation energy increased by Gd substitution. A two layer heterogeneous model consisting of semi-conducting grains divided by insulating grain boundary was capable to estimate the temperature and frequency dependent electrical properties of CFGO ceramics [62].

Farea *et al.* [63] reported the structural and electrical behavior of Cadmium substituted Co-ferrite. The sol-gel technique was used to prepare $Co_{0.5}Cd_xFe_{2.5-x}O_4$. The substitution of Cd improve the dielectric constant and loss tangent of Co-ferrite. The complex impedance spectroscopy analysis indicated the capacitive and resistive properties of the material is attributed due to the grain and grain boundary contribution.

Chen *et al.* [64] prepared Ni-Zn ferrite by Co-precipitation method. The grain size effect on the dielectric relaxation and magnetism was investigated in the ceramics. The non-Debye type relaxation phenomena was confirmed by the classic cole-cole plots. It was reported that the dielectric permittivity in the ferrite is associated to four types of polarization i,e interfacial, dipolar, ionic and electronic polarization, among which dipolar and interfacial polarization are sharply temperature dependent.

Conventional solid state chemical reaction method was used to prepare La doped Co-ferrite. Bharathi *et al.* [65] investigated the detail electrical and dielectric properties of the La doped Co-ferrite. The improvement of electrical and dielectric behavior was attributed to the structural changes induced by the doping La^{3+} for Fe^{3+} ions at B-site of the spinel ferrite. The dispersion of dielectric constant of the materials fitted to the modified Debye function. The temperature dependence electrical conductivity exhibits two regions corresponding to small polaron and variable range hopping mechanism.

The signature of ferroelectricity in the magnetically ordered Mo-substituted Cobalt ferrite was studied by Dwivedi *et al.* They used ceramic method to synthesize the sample and showed the coexistence of both magnetic and ferroelectric ordering in the materials. They also estimated the hopping energy of the material ~0.38eV at 290K [66].

Hashim *et al.* [67] showed the structural, electrical and magnetic properties of Copper doped Cobalt ferrite prepared by sol-gel method. The existence of normal Maxwell-Wagner type of dielectric dispersion because of interfacial polarization was inferred from dielectric study. From the study of impedance spectra they concluded that the conduction was through grain boundary. It was also reported that the magnetization was diminishes with cu-doping.

Kumar *et al.* [68] reported the FTIR and electrical behavior of Dy-doped Cobalt ferrite nano-particles. They reported that the material exhibits two absorption bands corresponding to two different sites in the spinel ferrite. The value of resistivity of the material was reported to be 10^5-10^9 ohm-cm.

The effect of LiO_2 doping on electrical behavior of $CoFe_2O_4$ was investigated by Selim *et al.* They inferred that the solid state interaction between Co_3O_4 and Fe_2O_3 to produce Co-ferrite is energetically easier by doping with small amount of LiO_2. Also the electrical parameters were noticeably affected by LiO_2 doping [69].

The temperature and frequency dependence of dielectric constant of Ni-Mg-Zn-Co ferrites was reported by Patil *et al.* They have used ceramic method to synthesize the sample. They have observed some peaks in the tangent loss curve and this was due to the matching of hopping frequency with the frequency external field [70].

Ishaque *et al.* [71] investigated the structural, electrical and dielectric behavior of Yttrium substituted Mg-ferrite. The double sintering ceramic technique was used to prepare the samples. A slight increase of lattice constant was observed for $MgY_{0.04}Fe_{1.96}O_4$. The resistivity of MYFO was significantly enhanced due to Y^{3+} ions. They reported that the dielectric constant was diminished with increment in Yttrium content and the frequency dependent of dielectric constant could be best described based on Maxwell-Wagner type of interfacial polarization in accordance with Koop's phenomenological theory.

Dar *et al.* [72] reported the dielectric and impedance study of polycrystalline Li-Cd-Ni ferrite synthesized by citrate-gel auto combustion method. They showed that the ac conductivity of the material increases with temperature and the conduction is due to correlated barrier hopping mechanism except for Li-Cd ferrite, which followed small polaron conduction method.

A series of Cerium doped Co-Ni ferrites were prepared using chemical co-precipitation and sol-gel auto combustion methods by Abbas *et al.* It was reported that the grain size was found to decrease while the density was increased with Ce-doping. The dielectric study confirmed the existence of Debye type relaxation process. They also reported the DC resistivity decreased from 10^8 (ohm-cm) to 10^6 (ohm-cm) at 373K with increase in Ce content [73].

Vaithyanathan *et al.* [74] investigated the detail structural and magnetic behavior of Sn and Ti doped Cobalt ferrite prepared by solid state reaction method. They studied the Raman spectroscopy which showed the peaks corresponding to tetrahedral and octahedral sites the substitution of massive Sn^{4+} ions was confirmed from the right shift of the peak. They reported the saturation magnetization was decreased from 80 emu/gm to 60 emu/m and 61 emu/gm with Ti and Sn doping respectively.

Hu *et al.* [75] explained the origin of anomalous magnetic properties in epitaxial Cobalt ferrite thin flim in terms of cation distribution of Co^{2+} ions and internal and external lattice strain effect. They showed that by varying the parameters, they could able to tune the symmetry and magnitude of the magnetic anisotropy.

Chemical co-precipitation technique was used by Ali *et al.* [76] to prepare Holonium substituted Co-ferrites. The showed that due to Ho^{3+} doping there was cubic magneto crystalline anisotropy and hence strong grain-grain interaction. They concluded that the investigated material could be used in PRM due to large value of coercivity ~1000 Oe.

Guo *et al.* [77] synthesized Sm doped Cobalt ferrite nanofibers by sol-gel route and investigated the structural and magnetic properties. They reported that at low temperature (500-700^{o}C) the $CoFe_{2-x}Sm_xO_4$ fibers were of single ferrite phase but at high temperature (800^{o}C) with relatively high concentration of Sm (0.15-0.20) the ferrite phase become unstable and the second phase of perovskite $SmFeO_3$ occurs. The grain size was decreased with increase in Sm content. They observed that the saturation magnetization and coercivity increased with crystalline size while decreased with Sm doping concentration.

The impact of Terbium substitution on the Cobalt ferrite nanoparticles was investigated by Sodaee *et al.* The pure Cobalt ferrite showed two sextets corresponds to iron ions occupying the A and B sites and strong preference of Tb^{3+} ion in the A site was seen. They also reported that the blocking temperature increased with Tb doping. They showed the temperature vs. susceptibility curves were well fitted with Vogel-Fulcher model. They proposed that adding Tb ion could enhance the saturation magnetization of Co ferrite which could make the material suitable for recording purpose [78].

Brown and Park [79] reported the magnetic resonance phenomenon in ferrites in 1954. They calculated the resonant frequency of rotations of domain magnetization in ferrimagnetic material using the molecular filed approximation and taken into account the effect of anisotropy and external field.

In 1955, Brown and Gravel [80] investigated the domain rotation in Nickel ferrite and showed that the initial permeability of Ni ferrite was due to domain rotation.

The effect of La^{3+} doping on the electrical, dielectric and magnetic properties of Cobalt ferrite was reported by Kumar *et al.* It was inferred that the doping of La^{3+} ions increased the dc resistivity (10^6 ohm-cm) which could make the ferrites suitable for high frequency application. The samples showed satisfying value of saturation magnetization and remanence at room temperature [81].

Murugesan *et al.* [82] reported the comparison of structural, dielectric and magnetic behavior of Cobalt ferrite synthesized by auto combustion method and ceramic route. The displayed the lattice constant of the samples was higher for the sample prepared by ceramic route. They also presented the values of saturation magnetization, coercivity and remanence were 42 emu/gm, 1553 Oe and 18.5 emu/gm for auto combustion method and 66.7 emu/gm, 379.6 Oe and 17.3 emu/gm respectively.

Magneto dielectric effect and magnetic field tunable dielectric resonance in Mn-Zn ferrite was presented by Chen *et al.* They showed that a magnetic field of 3.5 kOe induced a giant mageto dielectric response of 1800% at 7 MHz at room temperature [83].

Ceramic technique was taken to prepare Mn doped Ni-Zn ferrite by Dionne *et al.* in 1987 [84]. They investigated the magnetic properties of the material and found a square hysteresis loop. The Mn doping removed the stress sensitivity. It also lowered the saturation magnetization and Curie temperature.

Wang *et al.* in 1990 reported the electrical behavior of Zn ferrite [85]. They suggested that the conduction in Zn ferrites occurred by charge transport involving valance fluctuation on cations in octahedral site.

Algude *et al.* [86] synthesized Cr^{3+} doped Co-Zn ferrite by solid state reaction method. They studied the evidence of elastic behavior of the material by using ultrasonic phase technique. They displayed that the longitudinal and shear wave velocities were increased with Cr doping. Also reported that all the elastic modulus were increased due to Cr^{3+} ions in the B site of the material.

Significant effect of Mn doping on the magnetic and electrical properties of low temperature sintered Nickel-Zinc ferrite was reported by Yue *et al.* It was also reported that with increasing Mn content, the resonant frequency, dc resistivity, activation energy and the Curie temperature decreased, while initial permeability first increased, reached a maximum and then decreased [87].

The effect of grinding on the structural, magnetic and dielectric properties of Zn ferrite was presented by Shenoy *et al.* They studied the detail dielectric behavior and reported that the dielectric dispersion was because of interfacial polarization suggested by Koops. The Fe^{2+} ions produced electron hopping and the Oxygen ion vacancy in the lattice contributed to dielectric permittivity. The presence superparamagnetism in the ultrafine Zn ferrite was also reported [88].

Tantalum and Potassium doped Strontium-Calcium hexaferrites with pure magnetoplumbite phase was successfully synthesized by Ashiq *et al.* [89] using sol-gel combustion method. They found very high dielectric constant of the material which make the material applicable in microwave device. The value of coercivity of all the synthesized

samples was high enough (>6000 Oe) for their application in longitudinal magnetic recording media.

Peng *et al.* [90] reported the impact of Pr substitution on magnetic and dielectric properties Ni-Zn ferrite. They observed the lattice constant was first increased and then decreased. The curie temperature of the material was reported between 308-320^{o}C. The also showed the saturation magnetization diminished while the coercivity increased with Pr doping level.

Hsiang *et al.* [91] investigated the effect of Cobalt substitution on the dielectric behaviors of Cu-Zn ferrite, synthesized by solid state reaction technique. It have been seen that Co doping strongly affects the space polarization and dielectric behavior. The dielectric constant first increased with Co doping and then decreased.

Morphological, magnetic and dielectric behavior of Mg doped Ni ferrite ($Ni_{1-x}Mg_xFe_2O_4$) was reported by Moradmard *et al.* The spherical shape of pure Ni ferrite was confirmed from the FESEM micrograph. They found two absorption band from FTIR spectra corresponding to tetrahedral and octahedral site. The magnetic saturation was decreased while the coercivity increased with Mg^{2+} substitution [92].

Angadi *et al.* [93] observed the decreased of magnetic saturation, remanence decreased with increase in Sm^{3+}-Gd^{3+} concentration into Mn-Zn ferrite. They also showed the low value of dielectric constant and high tangent loss.

The detail microstructural and electrical behavior of Barium-Strontium Titanate and Ni-Zn ferrite composite was investigated by Pandya *et al.* They reported that the

dielectric dispersion of the samples obeyed the Maxwell-Wagner type of space polarization The showed that for {0.6(BST)+0.4(NZFO)}, the dielectric constant was exceptionally high and very low loss, offers a great promise for the composite for tunable frequency filter application [94].

Murugesan *et al.* [95] reported the reduction of crystalline size of Mn ferrite due to Gd^{3+} doping. The FTIR spectra showed two absorption band. They also showed the dielectric constant and ac conductivity increases with Gd substitution.

The structural and electrical behavior of Ni doped Mn-Zn nanoferrite was investigated by Chitra *et al.* They reported that the Mg-Mn-Ni nanoparticles have anti-bacterial activities and drug delivery properties. They also showed the high resistivity of the material [96].

Multiferroic and spinel ferrite composites of $\{(1-x)Bi_{0.7}Al_{0.3}Mn_{0.3}Fe_{0.7}O_3\text{-}xLi_{0.3}Zn_{0.4}Fe_{2.3}O_4\}$ were synthesized using the solid state method by Nazir *et al.* [97] and showed their structural, electrical and dielectric behavior. Each samples showed a metal to semiconductor transition. This may helpful in switching application.

Complex impedance and electrical modulus studies of Al doped Co-Cu-Zn ferrite was reported by Arjumanara *et al.* They clarified the dielectric study based on Verway de-Boer hopping mechanism, Maxwell-Wagner model and Koop's phenomenological theory. They showed the dominance of grain boundary in the conduction process [98].

Pandit *et al.* [99] presented the cation distribution controlled dielectric, electrical and magnetic properties of In^{3+} doped Cobalt ferrite. The material showed semiconductor

like conductivity behavior. They observed the resistivity of the samples was of the order of 10^6-10^9 ohm-cm and low dielectric constant which could be used in power transformer at high frequency.

The dielectric relaxation and conduction mechanism of Cobalt ferrite was studied by Panda *et al.* They concluded from the observation of temperature dependent of resistivity, ac conductivity and mobility that the material was semiconductor in nature. The ac conductivity was clarified based on overlapping large polaron tunneling model and small polaron was responsible for dc conductivity which was explained by Mott and Davis model [100].

Singh *et al.* [101] studied the CNFO-PLZT magneto electric composite for multiferroic applications. They stated that the dielectric constant increased with ferrite content. They also showed that the magnetic properties increased with ferrite concentration and the magneto electric coupling coefficient for 5% composite is 1.2 mV/(cm-Oe).

The dielectric and magnetic response of $SrFe_{12}O_{19}$-$CoFe_2O_4$ composite was studied by Hilczer *et al.* They showed the coupling of magnetic soft and hard phase in the composite. They showed that the composite exhibit very good dielectric and magnetic behavior [102].

Co-precipitation technique was used to prepare Ni-Zn ferrite nanoparticles by Saafan *et al.* They investigated the ac and dc conductivity of the materials. The samples showed the nature of soft superparamagnetism. They observed the semiconductor nature of the sample can be used in humid environmental applications [103].

Abo El Ata *et al.* [104] investigated the ac conductivity and dielctric behavior of $CoAl_xFe_{2-x}O_4$. They found that the quantum mechanical tunneling model was best to explain the conduction process in pure Cobalt ferrite while small polaron tunneling model was for Al doped Cobalt ferrite. The dielectric constant was decreased with Al content.

Elkestawy *et al.* [105] reported the ac conductivity and dielectric properties of Ti doped $CoCr_{1.2}Fe_{0.8}O_4$ spinel ferrite. They displayed very low value of conductivity along with small variation with frequency may made the ferrite a good candidate for practical applications. Also very low dielectric loss was observed for the material. They also investigated the ac conductivity and dielectric behavior of $Zn_{1-x}Cu_xCr_{0.8}Fe_{1.2}O_4$ spinel ferrite. The material showed semiconductor like conductivity behavior. The materials sowed very low conductivity and dielectric tangent loss at room temperature.

Mansour *et al.* [106] reported a correlative study of electric properties nano and bulk Mg-Mn spinel ferrite. They have seen that the conductivity and the dielectric constant of the bulk sample was higher compare to the nano sample.

The dielectric properties of Ti doped CO-Zn ferrite was investigated by Meaz *et al.* They used conventional ceramic method to synthesize the samples. The observed the increment of dielectric constant with Ti doping. They estimated the activation energy using the Arrhenius relation and found to be 0.256eV and 0.091eV for x=0.1 and 0.2 respectively [107].

The electric conduction mechanism in Nickel-Zinc ferrite was investigated by Abdeen *et al.* They observed that the ac and dc conductivity increased while the Curie

temperature and the activation energies decreased with Zn content. The activation energy in paramagnetic region was higher than that in ferrimagnetic region. They showed that the dispersion of ac conductivity satisfied The Jonscher's power law [108].

Chandrasekaran *et al.* [109] reported the studies of electric properties and FTIR spectroscopy of Al substituted Mn-Zn ferrite. They used conventional ceramic double sintering method to prepare the samples. They observed the grain boundary effect was dominant in the material. They found two major absorption band from FTIR spectra corresponding to the two sites of spinel ferrite.

The electrical and switching behavior of Al substituted Nickel ferrite was reported Patange *et al.* They have seen that the lattice constant decreased with Al concentration owing to Vegard's law. They concluded that the polaron hopping was liable for the conduction in the ferrites. They showed that the conductivity was switching between conduction and instability region in the initial phase [110].

El-Sayed *et al.* [111] investigated the electrical conductivity of Ni-Zn and Cr doped Ni-Zn ferrite. They reported that the Shottky defect could be deduced to prevail throughout the prepared samples indicated the presence of the amount of vacancies. They also showed that the electrical conductivity was first decreased with Zn content and then increased with further increase in Zn content.

The effect of Cu on the conductivity of Ni-Al ferrite was studied by Ata-Allah *et al.* They showed that the substitution of Cu in place of Ni in octahedral site leads to

existence of cation-cation interaction between Cu-Cu, which result in the increment of conductivity with increasing of Cu content [112].

Jonscher *et al.* [113] reported the theoretical evaluation of dielectric relaxation in solids. The dielectric relaxation of $A_xCo_{1-x}Fe_2O_4$ (A=Zn, Mg) mixed ferrite was investigated by Verma *et al.* They concluded from the dispersion of conductivity and permittivity that the dispersion was due to Maxwell-Wagner type of interfacial polarization. They found the minimum tangent loss was ~ 0.04 for the sample which could be applicable in microwave devices. The have studied the electric modulus properties of the material and found the existence of non-Debye type dielectric relaxation in the material [114].

Patil *et al*. [115] studied the dielectric behavior and ac conductivity in $Cu_xFe_{3-x}O_4$ ferrite. They reported that the temperature dependent of dielectric constant has abnormally high value at Curie temperature in $CuFe_2O_4$. They observed that the dielectric relaxation frequency shifted towards higher frequency as temperature increases in non-stoichiometric Cu-ferrite (x=0.8 & 0.6).

Dielectric properties and electric conductivity of Sm^{3+} substituted Mg-Zn ferrite was reported in detail by Melagiriyappa *et al*. They showed that the dielectric constant and loss tangent diminishes while the conductivity increased with raise in frequency at a certain temperature. They also reported that both the dielectric constant and ac conductivity increased with Zn content, reached a maximum value at x=0.6 and then decreased [116].

Hiti *et al*. [117] investigated the conductivity behavior Zn-doped Ni-Mg ferrites. They found that the Curie temperature and activation energy in both ferrimagnetic and paramagnetic region decreased with Zn substitution.

The ac conductivity and dielectric properties of Tb^{3+} doped $Ni_{0.4}Zn_{0.6}Fe_2O_4$ nanoparticles were clearly reported by Jacob *et al*. They found that the lattice constant was increased with Terbium content but after a particular concentration it was decreased. They suggested that the conduction was because of small polaron hopping in the material [118].

Khandekar *et al.* [119] investigated the effect of calcination temperature on the structural and electrical behaviors of Cobalt ferrite. The variation of dc resistivity suggested that the samples were magnetic semiconductors. Also the ac conductivity variation of the material suggested that the conduction was because of small polaron hopping in the material.

Ponpandian *et al.* [120] reported the electrical conductivity and dielectric properties of nano-crystalline Ni-ferrites. They showed that the impedance spectra exhibit two semicircles corresponds to grain and grain boundary contribution for 8 *nm* and 12 *nm* samples. They found the activation energy increased with grain size reduction due to blocking nature of grain boundary and lattice imperfections.

Gopalan *et al.* [121] showed the evidence of polaron conduction in Mg ferrite. It have been seen that the saturation magnetization of nano sized Mg ferrite was less than that of its bulk counterpart. They showed that the conduction was due to Maxwell-Wagner

interfacial polarization in agreement with Koop's phenomenological theory. The distribution of relaxation time provides enough evidence for existence of multiple equilibrium state in the system.

The finite size effect on the electrical properties of sol-gel synthesized Co ferrite powders was investigated in detail by George *et al.* The high dielectric constant at high temperature was clarified as because of the existence of permanent dipole moments, pointing a small effective charge separation. They found that the particle size was raised with the sintering temperature while the porosity of the materials decreased [122].

Farea *et al.* [123] studied the effect of frequency, temperature and composition on electrical characteristics of polycrystalline $Co_{0.5}Cd_xFe_{2.5-x}O_4$ ferrites. They found the decrement of dielectric constant, tangent loss ac conductivity with frequency and increment with temperature. They also investigated the influence of Ti doping on the electrical and magnetic properties of $Mn_{1+x}Fe_{2-2x}Ti_xO_4$ ferrite [124]. It was concluded that the ac conductivity was the increasing fluctuation of frequency and temperature. They showed the conduction in the material was due to correlated barrier hopping process.

Magnetic and dielectric properties of mixed spinel Ni-Zn ferrite was studied by Kambale *et al*. The saturation magnetization was seen to be raised with Ni concentration. The maximum resistivity was obtained from x=0.5 [125].

Hankare *et al*. [126] investigated the magnetic and dielectric properties of nano-crystalline Zn doped Cu-Mn ferrite. Magnetic measurements showed that the saturation

magnetization increased up to $x \leq 0.25$ and then decreased with further increasing Zn content. They also showed that the conduction was due grain boundary contribution only.

Magnetic and electrical behavior of Indium doped Cobalt ferrites was reported in detail by Nongjai *et al.* They showed that the grain size decreased while the lattice constant, porosity and specific surface area increased due to In doping. They concluded that high resistivity and low dielectric loss led the materials suitable for power application at high frequency [127].

The technique of ac conduction in nanostructured Mn-Zn mixed ferrites was successfully explained by Gopalan *et al.* They found that the ac conductivity decreased with increase in Zn content which suggested that the increase of activation energy due to Zn doping. The activation energy revealed that the conduction was governed by the hopping of polaron [128].

Hashim *et al.* [129] explained the influence of Cr^{3+} ions on the structural, electrical conductivity and magnetic behavior of Ni-Mg ferrites. They found that the dielectric constant and loss factor decreased with frequency. FTIR spectral studies showed the presence of two vibrational band corresponds to A and B site of the material. They also found the superparamagnetic blocking temperature was increased with Cr-substitution.

Magnetic and electrical properties of Cobalt nano ferrite was investigated by Golapan *et al.* They found maximum M_r/M_s value to be 0.82 which indicate the contribution of cubic anisotropy in the material. They also showed that the ac conductivity is due to small polaron tunneling [130].

Ahmed *et al.* [131] reported the structural and electrical studies on La^{3+} doped Ni-Zn ferrites. They reported that for small Zn concentration A-B interaction was predominant because of the existence of magnetic ions in both A and B site, though for high Zn concentration B-B interaction began to dominate. They also showed a strong correlation between conduction mechanism and dielectric behavior .The change of thermo-electric power with temperature affirmed that the increase in conductivity is because of raisingin carrier mobility, not due to the thermal creation of carriers.

The magnetic and electrical behavior of Co-Ni-Mn ferrite was investigated by Shaikh *et al.* Saturation magnetization was decreased with increase in Ni content. Also reduction in coercivity was seen which showed the material was suitable for magnetic recording media with some improvement [132].

Pradeep *et al.* [133] investigated the structural, magnetic and electrical properties of nano-crystalline Zn ferrite. They showed the ferrimagnetic behavior of Zinc ferrite characterized with relatively high saturation magnetization and coercivity values. The conductivity study showed that the ferrimagnetic exchange interaction hinder conduction process, while the paramagnetic phase supported it due to absence of exchange interaction.

Studies of ac conductivity and initial magnetic permeability of rare earth substituted Li-Co ferrites was some by Abo El Ata *et al.* [134] the ac conductivity showed dispersion with frequency at low temperature and it obeyed the universal power law. They reported that the the conduction was due the classical barrier hopping mechanism.

Pradhan *et al.* [135] explained the structural, electrical and transport properties of Ni-Zn ferrite. They showed that the bulk conductivity was originated from variable range hopping of localized polarons. They established the equivalance of polaron conduction and high permittivity of Ni-Zn ferrite. They also reported that the frequency dependent of ac conductivity behavior satisfied the Jonscher's power law and was clarified by utilizing jump relaxation model.

The electrical conductivity of Cobalt doped Mg-Mn nanoferrite was studied by Kumar *et al.* They found that the dc resistivity was reduced with increment in temperature. The impedance analysis showed the conduction was due to contribution of grain boundary. The pure Mg-Mn ferrite showed remarkably higher value of dielectric constant [136].

Pradhan *et al.* [137] correlated the dielectric, electric and magnetic behavior near magnetic transition temperature of Cobalt-Zinc ferrite. The dielectric constant was found to be increased with frequency while loss tangent decreased. They showed the Cole-Cole plot which was associated with only one semi-circle which confirmed the existence of non-Debye type relaxation process. They also showed that frequency ac conductivity satisfied the Jonscher's single power law.

Ac electrical conductivity of Ni-Mg ferrite was reported by Hiti *et al.* They reported that the Curie temperature and activation energy was reduced with increment in Ni content. The activation energy in paramagnetic region was observed to be higher than that in ferrimagnetic region. They also established empirical formulae for temperature reliance of power and coefficient of frequency in single power law [138].

Temperature and frequency dependence of ac electrical properties of Zn and Ni doped $CoFe_2O_4$ was successfully investigated by Mandal *et al.* They showed that the reliance of dielectric constant with frequency support the Rabinkin and Novikova theory for polarization. Furthermore, the complex impedance was found to decrease with temperature due to temperature dependent electrical relaxation process. They also reported that the conduction was because of large polaron hopping mechanism [139].

Rahman *et al.* [140] reported the semiconductor to metallic transition and polaron conduction in nanostructured Cobalt ferrite. They found that both grain and grain boundaries contribute to the conductivity of the material. They observed semiconductor to metal transition was at ~330K in Cobalt ferrite. They concluded that the strong C-C interaction was responsible for this type of transition.

Batoo *et al.* [141] studied the effect of temperature on electrical behavior of nano-crystalline Ni-Cd ferrites. Complex impedance spectra displayed only one semi-circle corresponds to grain boundary contribution. They found that ac conductivity increased with increase in grain size. They also reported the anomalous behavior of dielectric constant with frequency at different temperature.

The effect of Cu doping on the electrical and magnetic properties of $NiFe_2O_4$ was studied by Patil *et al.* The dielectric constant, loss tangent, electrical resistivity and activation energy was fund to increase with Copper concentration. They also reported that the saturation magnetization and coercivity was increased with Cu content which explained by the fact that, being John-Teller, Cu ion leads to improve the lattice distortion [142].

Devan *et al.* [143] successfully investigated the effect of Cobalt substitution on different properties of Ni-Cu ferrites. They showed that the value of Seebeck coefficient (α) and the ac conductivity suggest that the conduction might be due to the polaron hopping mechanism. Since the dielectric constant is inversely proportional to resistivity, it showed the decreasing trend with Co content.

Ajmal *et al.* [144] investigated the ac conductivity and magnetic behavior of Ni-Zn ferrite. They showed that the value of ac conduction ($ln\sigma_{ac}$) increased from -7987 S/m to -0.020 S/m with increase in Zn content from 0.0 to 0.1 at 1 MHz. All the sample followed Maxwell-Wagner polarization. The saturation magnetization varied from 196.459 emu/g to 0.330 emu/g. This might be due to non-magnetic nature of Zinc.

1.15 Aim of Present Work

The aims of the present work are as follows

- To prepare the series of Mo doped Co-Zn ferrite with the help of solid state reaction method.
- To characterize all the sample for the structure by using the high resolution X-ray diffraction (HRXRD) technique.
- To investigate the dielectric, impedance spectroscopy, electrical conductivity and magnetic behavior of all the sample.